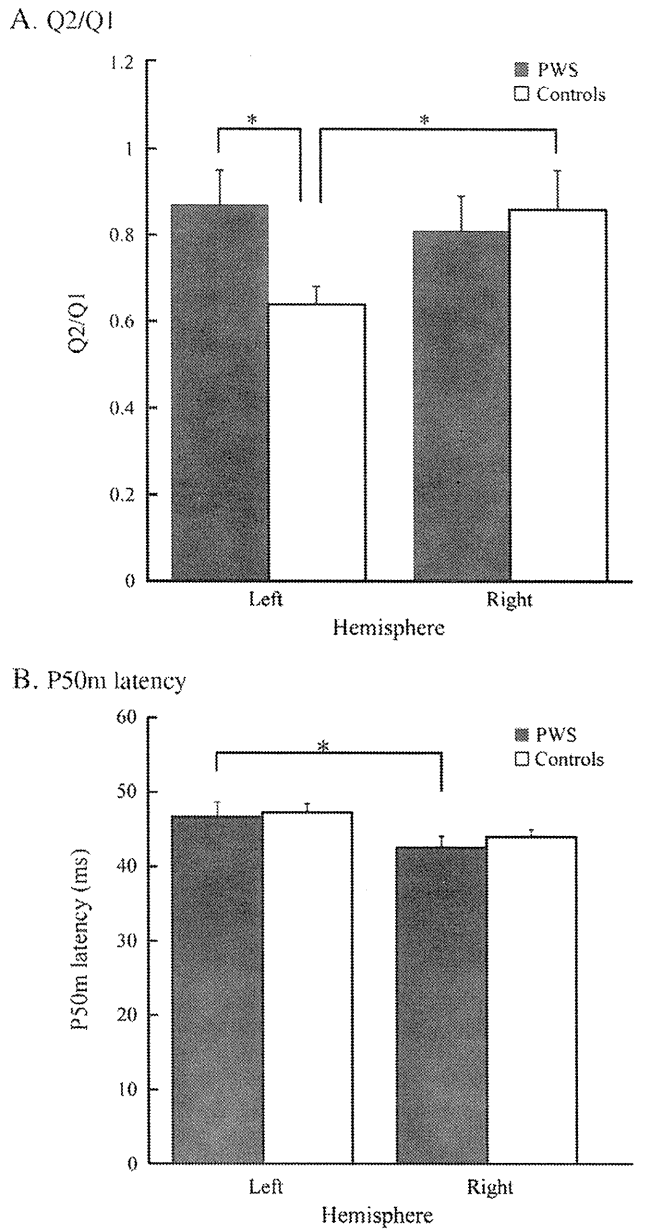


**Fig. 2.** (A) P50m auditory sensory gating ratios (Q2/Q1) in controls and PWS in the left and right hemispheres. The left gating ratio in PWS is significantly larger than that in the controls. The left gating ratio in controls is significantly smaller than the right gating ratio. (B) P50m latency in controls and PWS in the left and right hemispheres. The right S1 latency is significantly shorter than the left S1 latency in PWS. Error bars represent SEM. *$p<0.05$.

effect of group was not significant [$F(1, 25)=1.45$, $p=0.239$], a significant interaction between group and hemisphere was found [$F(1, 25)=4.458$, $p=0.022$]. A post-hoc analysis revealed that there was a significant difference between the 2 groups on the right side ($p=0.039$) but not in the left hemisphere. This indicates that the N100m in PWS is located more anteriorly than that in the controls (Fig. 5A). In both controls and PWS, the right N100m is located more anteriorly than the left N100m ($p=0.018$ and $p<0.001$, respectively). The interaction between group and frequency was also significant [$F(2, 24)=4.458$, $p=0.022$]. Post-hoc tests revealed that there was a significant difference among each frequency in PWS, whereas 250 Hz was not different from 1000 Hz in the controls.

The slope of the y axis regression line of the right hemisphere was considerably steeper for PWS than for the controls ($p=0.040$) (Fig. 5B), indicating that the tonotopic map in the right hemisphere of PWS was larger than that in the controls. The correlation between the tonotopic map expansion and the stuttering rate was, however, not significant.

Regarding the x coordinate (medial–lateral axis), a significant main effect of frequency was found [$F(2, 26)=5.472$, $p=0.01$]; however, there was no significant difference between the 2 groups. Similarly, there was no significant difference between the 2 groups for the z coordinate.

For N100m latency, there were significant main effects of frequency [$F(2, 26)=203$, $p<0.001$] and hemisphere [$F(1, 27)=6.635$, $p=0.015$]. The interaction between hemisphere and frequency was also significant [$F(1, 27)$, $p=0.004$]. Post-hoc analysis revealed that the latency at 250 Hz was significantly longer than that at 4000 Hz ($p<0.001$) and 1000 Hz ($p<0.001$). The N100m latency at 250 Hz in the left hemisphere was shorter than that in the right hemisphere ($p<0.001$). No significant group difference was observed. There was also a main effect of frequency on the N100m dipole moment strength ($p<0.001$); however, there was no significant difference between the 2 groups.

*Experiment 3: Voxel-based morphometry*

VBM analysis revealed 4 significant clusters of increased GM volume and 3 significant clusters of decreased GM volume in PWS (Table 3). Compared with the controls, PWS showed significant increases in GM volume in the right STG (BA42, Fig. 4C), right inferior frontal gyrus (BA47), right insula (BA13), and right supramarginal gyrus (BA40). Conversely, decreases in GM volume were observed in the left precentral gyrus, left middle frontal gyrus (L), and left insula (BA13). There was no significant decrease in GM volume in the left STG, left inferior frontal gyrus, medial frontal gyrus, and left supramarginal gyrus.

## Discussion

We examined spatiotemporal signatures of the basic auditory system by using an auditory sensory gating paradigm and tonotopic maps with MEG and determined structural volumes by using VBM. The new findings of this study are summarized as impaired auditory sensory gating in the left hemisphere, functional map expansion of the right STG, and greater asymmetric tonotopic organization in PWS. We also found left-lateralized auditory sensory gating in normal controls.

*PWS cannot "gate out"*

Sensory gating involves the ability to both "gate in" relevant information and "gate out" irrelevant information. A lack of P50m (or P50) suppression has been proposed as the index of abnormal auditory sensory gating (or "gate out") in schizophrenia (Adler et al., 1982; Thoma et al., 2003; Hirano et al., 2010) and Alzheimer's disease (Jessen et al., 2001). We first demonstrated the left hemispheric impairment of P50m suppression in PWS; this finding indicates that the normally present inhibitory mechanisms are markedly reduced in PWS and supports our working hypothesis that PWS cannot gate out ignorable auditory inputs, which lead to errors. The observed P50m responses are located on both sides of the superior temporal gyri close to Heschl's gyrus, consistent with the findings of previous studies in non-stuttering subjects (Onitsuka et al., 2000; Lu et al., 2007; Hirano et al., 2008).

The phenomenon of sensory gating in PWS has previously been studied using EEG (Özcan et al., 2009). Özcan et al. (2009) examined the P50 suppression recorded from the vertex (Cz) and found no difference between PWS and controls. Auditory sensory gating in EEG is derived from at least 2 distinct generators, namely, the tangential component of the auditory cortex and the radial component of the

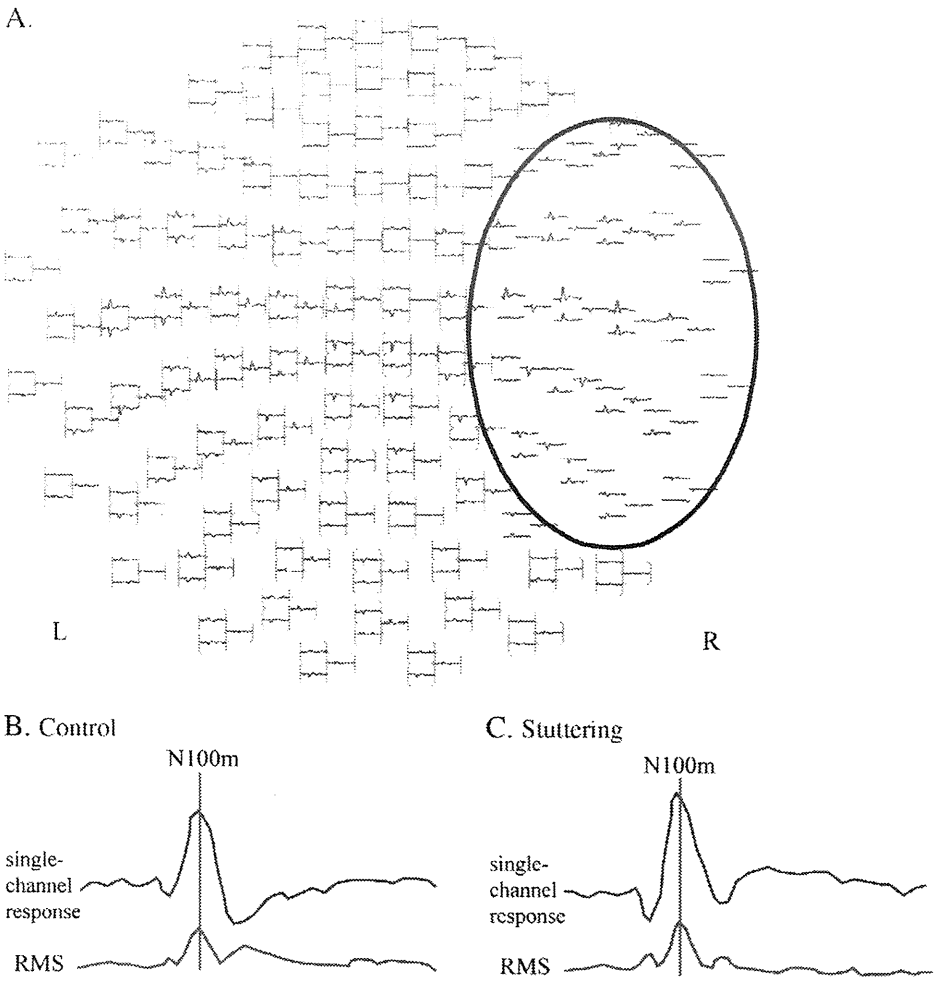


**Fig. 3.** Source of the N100m response estimated by MEG. Seventy channels around the N100m peak in the right hemisphere (encircled) were used to fit a single dipole source (A). Single-channel response and RMS over the selected channels in a representative control (B) and a representative stuttering (C) subject. No significant difference was observed between the N100m dipole moments of the 2 groups.

frontal cortex (Weisser et al., 2001; Korzyukov et al., 2007). Although scalp EEG is sensitive to both tangential and radial components of current sources in a spherical volume conductor, MEG detects only the tangential component. MEG therefore measures activity in the sulci selectively, whereas scalp EEG measures activity in both the sulci and at the top of the cortical gyri, but appears to be influenced to a greater extent by radial sources (Cohen and Cuffin, 1983). Thus, it is likely that the results of our MEG study differed from those of a previous EEG study of sensory gating in PWS (Özcan et al., 2009). Our study is notable in that unlike in the studies mentioned above, we found that auditory sensory gating in the left hemisphere is dysfunctional in PWS.

Interestingly, in the controls, the Q2/Q1 ratio for the left hemisphere was significantly smaller than that for the right hemisphere, which indicates that sensory gating in the left auditory cortex is more dominant than that in the right auditory cortex. Such asymmetry in auditory sensory gating was not found in PWS. The left hemispheric specificity of gating in normal controls has not previously been reported. We suggest 3 possibilities that might explain this unexpected result. First, the left Q2/Q1 ratio in the controls in our study is almost comparable to that of previous MEG studies (Weiland et al., 2008; Hirano et al., 2010). Unlike the findings of previous studies, the left Q2/Q1 was also significantly lower than the right Q2/Q1 ratio; this finding can be attributed to binaural stimulation (Hirano et al., 2010; Lu et al., 2007; Hanlon et al., 2005; Thoma et al., 2003). The brain regions associated with language are left-sided in healthy right-handers (Knecht et al., 2000). Thus, it is plausible that auditory sensory gating is left-lateralized. Second, we used strictly monaural stimulation for each ear separately so as not to induce cross-hearing. Most P50m suppression studies involve binaural stimulations or stimulations at a high sound pressure level to induce cross-hearing (Thoma et al., 2003, 2004; Edgar et al., 2003, 2005; Lu et al., 2007; Weiland et al., 2008; Hirano et al., 2008, 2010). Third, since it is well known that P50 is affected by vigilance (Cullum et al., 1993), we used silent movies to keep the subjects awake. Thus, the interhemispheric difference in auditory sensory gating in males could be evaluated more precisely in our study population.

*Altered tonotopy in PWS*

We first demonstrated expansion of the tonotopic representations in the right hemisphere of PWS. The auditory cortex is tonotopically organized in humans, such that higher frequencies are represented medially and posteriorly (Pantev et al., 1989, 1998b). When N100m dipole locations are plotted against the logarithm of frequency, they can be represented by a straight line (Pantev et al., 1995). The steeper the slope of this regression line, the more extended is the map of tonotopic representation (Elbert et al., 2002). Our results showed that the slope of the y-axis regression line of the right hemisphere was considerably steeper for PWS than for the controls, indicating that the tonotopic map of PWS was expanded in the right auditory cortex. The

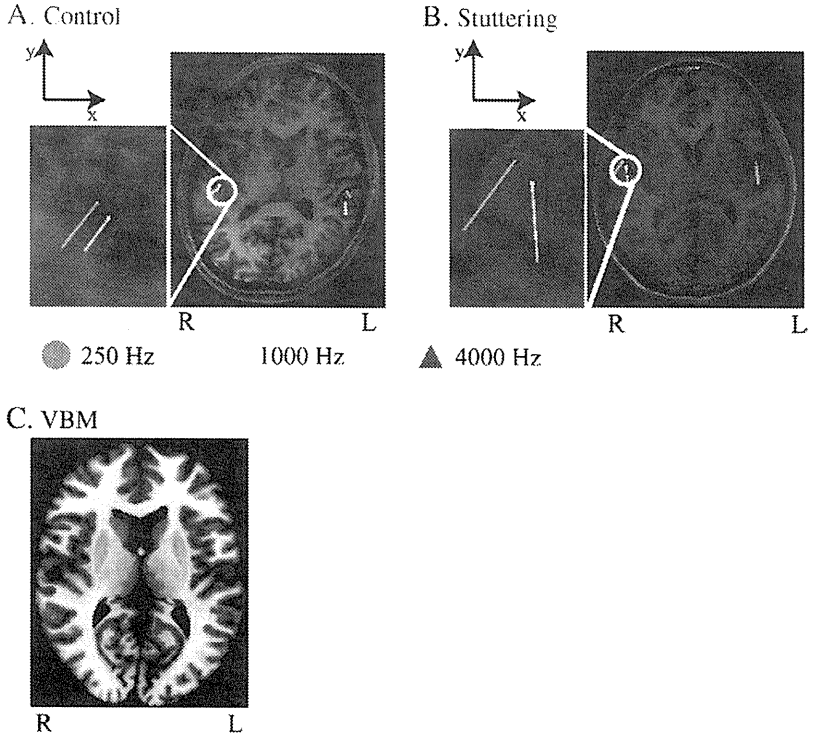


**Fig. 4.** N100m sources for 3 tonal frequencies overlaid on MRI in the same control (A) and stuttering (B) subjects. Note that tonotopic organization in the right but not in the left hemisphere is enlarged in the stuttering subject (see right enlarged image). In the VBM result (C), the red patches in the right STG show statistically more significant increments in PWS than in controls and are overlaid onto a standard T1 template in MRIcron (http://www.sph.sc.edu/comd/rorden/mricron/).

expansion of tonotopic representation could be ascribed to use-dependent cortical plasticity (Bakin and Weinberger, 1990; Elbert et al., 2002). Elbert et al. (2002) demonstrated auditory cortical plasticity attributable to expansion of the N100m tonotopic map in blind subjects who had to rely on nonvisual, primarily auditory, input. N100m tonotopic organizations have been generated from the secondary auditory cortex, which mirrored the tonotopic organization in the primary auditory cortex (Pantev et al., 1995). In a structural assessment using VBM, we demonstrated an increased volume of GM in the right STG near the N100m tonotopic organization. We also found that the N100m of the right hemisphere in PWS was more anterior than that in the controls, which could be related to the expansion of tonotopic representation. Taken together, these observations suggest that structural cortical plasticity could be induced in the right STG in PWS, which is in accordance with functional expansion of the tonotopic representation.

We found both functional and structural changes in the right STG. Kell et al. (2009) showed functional overactivation in the right primary auditory cortex during speech. The following structural changes in the right auditory cortex have been reported in previous studies: reduced right–left asymmetry (Foundas et al., 2001), increased white matter (Jäncke et al., 2004), and alterations in the structure of the right-sided perisylvian region (Cykowski et al., 2008). To date, the relation between function and structure of the right auditory cortex is unclear, but our study revealed that the function of the right auditory cortex is related to structural changes.

Although there have been many VBM studies of PWS (Jäncke et al., 2004; Beal et al., 2007; Chang et al., 2008; Kell et al., 2009; Lu et al., 2010), there exist considerable methodological differences among studies, and previous studies did not always reproduce the results of former studies. The results of our study did not replicate the changes of increased left STG (Beal et al., 2007). However, Lu et al. (2010) found that the GM volume in the left STG in PWS was lower than that in the controls. Therefore, it is evident that no reproducible changes in the left STG were found in PWS. Chang et al. (2008) did not report lateralized decreased GM volume; however, Kell et al. (2009) found left-lateralized decrease in GM volume (e.g., inferior frontal gyrus, medial temporal gyrus, and supramarginal gyrus) in PWS but no increase in GM volume in the right hemisphere. Thus, our VBM results are partly consistent with those of Kell et al. (2009).

**Table 2**
The 3D mean source locations of N100m (mm).

| Frequency | Dimension | PWS | | Controls | |
|---|---|---|---|---|---|
| | | Left | Right | Left | Right |
| 250 Hz | x | −54.8 ± 1 | 52.5 ± 1.2 | −52.5 ± 1.3 | 53 ± 0.7 |
| | y | 5.8 ± 1.6 | 13.6 ± 2 | 4.9 ± 1.3 | 7.4 ± 1.4 |
| | z | 53.3 ± 2.4 | 49.5 ± 2 | 56.4 ± 1.2 | 53.2 ± 1.6 |
| 1000 Hz | x | −54 ± 0.7 | 50.7 ± 1.1 | −51.8 ± 1.3 | 52.7 ± 0.8 |
| | y | 4.4 ± 2.3 | 12.5 ± 1.7 | 4.4 ± 1.4 | 8.5 ± 1.3 |
| | z | 51.8 ± 2.3 | 49.8 ± 1.7 | 55.9 ± 1.4 | 52.8 ± 1.4 |
| 4000 Hz | x | −51.6 ± 1.3 | 50.3 ± 1.2 | −48.9 ± 1.6 | 52.4 ± 0.9 |
| | y | 1.8 ± 2.4 | 9.1 ± 1.9 | 1.8 ± 1.3 | 6.5 ± 1.2 |
| | z | 52.1 ± 2.3 | 50.3 ± 1.8 | 54.7 ± 1.2 | 53.6 ± 1.4 |

x: medial–lateral, y: anterior–posterior, z: superior–inferior.

*Defect of auditory–motor integration*

We have demonstrated the left hemispheric impairment of P50m suppression in PWS. This indicates that PWS cannot gate out ignorable auditory inputs, which in turn cause auditory error signals. Since the P50m suppression paradigm was inattention and an early response of 50-ms latency without cognition, auditory sensory gating is believed to work automatically. Auditory error signals from impaired auditory sensory gating could cause abnormal auditory feedback. Max et al. (2004) assumed that stuttering would derive from a mismatch between

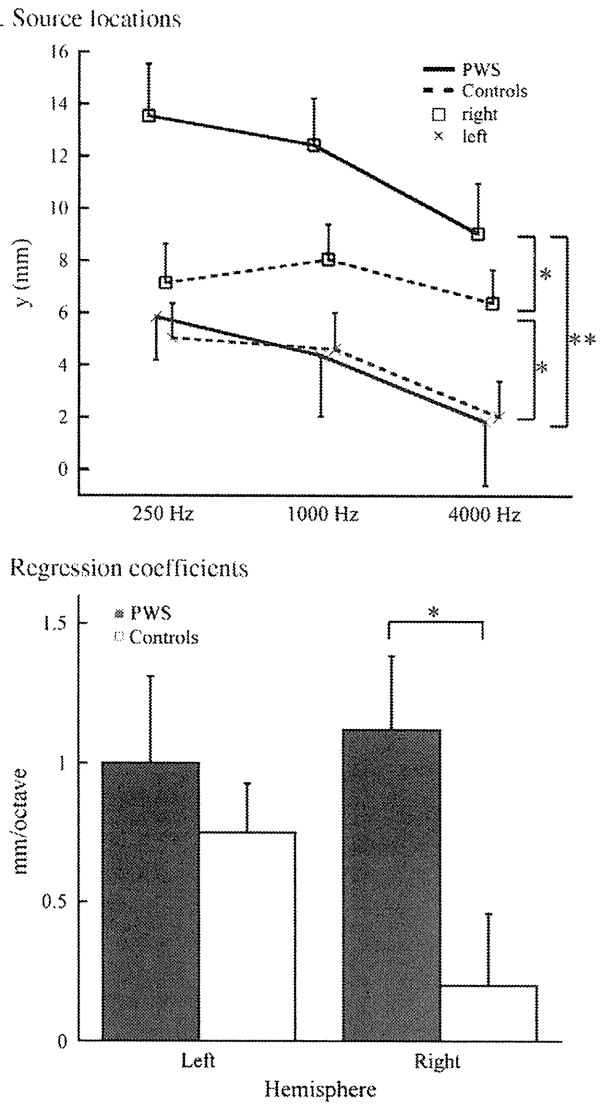


**Fig. 5.** Source locations along the y axis (anterior–posterior) as a function of stimulus frequency (mean ± SEM) (A). There is a significant difference between PWS and controls in the right hemisphere. The sources of higher frequencies are located more posteriorly as a tonotopic arrangement. The regression coefficient of the y axis in each group (B). The tonotopic map for PWS was larger than that for controls on the right side. *p<0.05, **p<0.01.

**Table 3**
Regions, coordinates, and t-statistics of significantly different gray matter voxels in VBM.

| Region | BA | x | y | z | t-value |
|---|---|---|---|---|---|
| *PWS > controls* | | | | | |
| Superior temporal gyrus (R) | 42 | 60 | −25 | 10 | 3.72 |
| Inferior frontal gyrus (R) | 47 | 54 | 31 | −14 | 4.26 |
| Insula (R) | 13 | 44 | 20 | 7 | 4.07 |
| Supramarginal gyrus (R) | 40 | 54 | −36 | 39 | 4.08 |
| *Controls > PWS* | | | | | |
| Precentral gyrus (L) | 6 | −33 | −9 | 51 | 5.64 |
| Middle frontal gyrus (L) | 11 | −23 | 42 | −7 | 3.81 |
| Insula (L) | 13 | −41 | 13 | 15 | 3.72 |

BA: Brodmann area.
x, y, and z represent medial–lateral, anterior–posterior, and superior–inferior axes, respectively.

predicted motor commands (feedforward) and auditory and somatosensory (feedback) consequences of the executed movements (speech). This mismatch could result in an increased need for feedback-based corrections but would make worse by abnormal auditory feedback.

Chang et al. (2009) demonstrated that PWS had less activation than controls in the left STG but greater activation in the right STG. Kell et al. (2009) inferred that the compensatory effect of auditory feedback integration in the motor program is manifested via right auditory cortex activation. If defects in left auditory sensory gating induce some errors during auditory inputs in the left STG, PWS should show reduced auditory inputs in the left hemisphere and compensate by increasing auditory inputs from the right hemisphere. Increased auditory inputs from the right hemisphere could result in expansion of the tonotopic map. The expansion of tonotopic organization can occur under conditions of use-dependent plasticity, as seen in musicians (Pantev et al., 1998a, 2001; Gaser and Schlaug, 2003) and blind subjects (Elbert et al., 2002). The expansion of the tonotopic map could increase GM volume in the right STG. Cortical thickness can increase to compensate for impaired brain function. For example, an increase in cortical thickness was observed in the ipsilateral sensorimotor cortex of chronic stroke patients with subcortical lesions (Schaechter et al., 2006). Close functional coupling between the right and left auditory cortices is well known (Brancucci et al., 2005; Mukamel et al., 2005). Therefore, we consider the defect of left auditory sensory gating as one of the causes underlying an increase in the volume of the right auditory cortex. Taken together, we believe that the defective auditory–motor integration is the neural basis of stuttering.

## Conclusions

Our study demonstrated that the disturbed auditory sensory gating in the left hemisphere is an electrophysiological signature of stuttering, which reflects an inability of PWS to gate out unnecessary auditory information and the consequent stuttering. We also indicated an increase in GM in the right auditory cortex corresponding to the expansion of tonotopic organization. Our findings further suggest that altered auditory information processing provides a clue about stuttering pathophysiology.

## Acknowledgments

This work was supported by a Grant-in-Aid for Japan Society for the Promotion of Science (JSPS) Fellows (Y. K.) and by a Grant-in-Aid for Young Scientists (B) (K. O.).

## References

Adler, L.E., Pachtman, E., Franks, R.D., Pecevich, M., Waldo, M.C., Freedman, R., 1982. Neurophysiological evidence for a defect in neuronal mechanisms involved in sensory gating in schizophrenia. Biol. Psychiatry 17, 639–654.
Altrows, I.F., Bryden, M.P., 1977. Temporal factors in the effects of masking noise on fluency of stutterers. J. Commun. Disord. 10, 315–329.
Ashburner, J., 2007. A fast diffeomorphic image registration algorithm. Neuroimage 38, 95–113.
Bakin, J.S., Weinberger, N.M., 1990. Classical conditioning induces CS-specific receptive field plasticity in the auditory cortex of the guinea pig. Brain Res. 536, 271–286.
Beal, D.S., Gracco, V.L., Lafaille, S.J., De Nil, L.F., 2007. Voxel-based morphometry of auditory and speech-related cortex in stutterers. NeuroReport 18, 1257–1260.
Beal, D.S., Cheyne, D.O., Gracco, V.L., Quraan, M.A., Taylor, M.J., De Nil, L.F., 2010. Auditory evoked fields to vocalization during passive listening and active generation in adults who stutter. Neuroimage 52, 1645–1653.
Brancucci, A., Babiloni, C., Vecchio, F., Galderisi, S., Mucci, A., Tecchio, F., Romani, G.L., Rossini, P.M., 2005. Decrease of functional coupling between left and right auditory cortices during dichotic listening: an electroencephalography study. Neuroscience 136, 323–332.
Chang, S., Erickson, K.I., Ambrose, N.G., Hasegawa-Johnson, M.A., Ludlow, C.L., 2008. Brain anatomy differences in childhood stuttering. Neuroimage 39, 1333–1344.
Chang, S., Kenney, M.K., Loucks, T.M., Ludlow, C.L., 2009. Brain activation abnormalities during speech and non-speech in stuttering speakers. Neuroimage 46, 201–212.
Cohen, D., Cuffin, B.N., 1983. Demonstration of useful differences between magnetoencephalogram and electroencephalogram. Electroencephalogr. Clin. Neurophysiol. 56, 38–51.

Conture, E., 2001. Stuttering: Its Nature, Diagnosis and Treatment. Allyn & Bacon, Needham Heights, MA.
Cullum, C.M., Harris, J.G., Waldo, M.C., Smernoff, E., Madison, A., Nagamoto, H.T., Griffith, J., Adler, L.E., Freedman, R., 1993. Neurophysiological and neuropsychological evidence for attentional dysfunction in schizophrenia. Schizophr. Res. 10, 131–141.
Cykowski, M.D., Kochunov, P.V., Ingham, R.J., Ingham, J.C., Mangin, J.F., Riviere, D., Lancaster, J.L., Fox, P.T., 2008. Perisylvian sulcal morphology and cerebral asymmetry patterns in adults who stutter. Cereb. Cortex 18, 571–583.
Cykowski, M.D., Fox, P.T., Ingham, R.J., Ingham, J.C., Robin, D.A., 2010. A study of the reproducibility and etiology of diffusion anisotropy differences in developmental stuttering: a potential role for impaired myelination. Neuroimage 52, 1495–1504.
De Nil, L.F., Kroll, R.M., Lafaille, S.J., Houle, S., 2003. A positron emission tomography study of short- and long-term treatment effects on functional brain activation in adults who stutter. J. Fluency Disord. 28, 357–380.
Decker, T.N., Healey, E.C., Howe, S.W., 1982. Brainstem auditory electrical response characteristics of stutterers and nonstutterers: a preliminary report. J. Fluency Disord. 7, 385–401.
Edgar, J.C., Huang, M.X., Weisend, M.P., Sherwood, A., Miller, G.A., Adler, L.E., Canive, J.M., 2003. Interpreting abnormality: an EEG and MEG study of P50 and the auditory paired-stimulus paradigm. Biol. Psychol. 65, 1–20.
Edgar, J.C., Miller, G.A., Moses, S.N., Thoma, R.J., Huang, M.X., Hanlon, F.M., Weisend, M.P., Sherwood, A., Bustillo, J., Adler, L.E., et al., 2005. Cross-modal generality of the gating deficit. Psychophysiology 42, 318–327.
Elbert, T., Sterr, A., Rockstroh, B., Pantev, C., Muller, M.M., Taub, E., 2002. Expansion of the tonotopic area in the auditory cortex of the blind. J. Neurosci. 22, 9941–9944.
Foundas, A.L., Bollich, A.M., Corey, D.M., Hurley, M., Heilman, K.M., 2001. Anomalous anatomy of speech-language areas in adults with persistent developmental stuttering. Neurology 57, 207–215.
Fox, P.T., Ingham, R.J., Ingham, J.C., Hirsch, T.B., Downs, J.H., Martin, C., Jerabek, P., Glass, T., Lancaster, J.L., 1996. A PET study of the neural systems of stuttering. Nature 382, 158–162.
Gaser, C., Schlaug, G., 2003. Brain structures differ between musicians and non-musicians. J. Neurosci. 23, 9240–9245.
Giraud, A.L., Neumann, K., Bachoud-Levi, A.C., von Gudenberg, A.W., Euler, H.A., Lanfermann, H., Preibisch, C., 2008. Severity of dysfluency correlates with basal ganglia activity in persistent developmental stuttering. Brain Lang. 104, 190–199.
Hämäläinen, M., Hari, R., Ilmoniemi, R.J., Knuutila, J., Lounasmaa, O.V., 1993. Magnetoencephalography — theory, instrumentation, and applications to noninvasive studies of the working human brain. Rev. Mod. Phys. 65, 413–497.
Hampton, A., Weber-Fox, C., 2008. Non-linguistic auditory processing in stuttering: evidence from behavior and event-related brain potentials. J. Fluency Disord. 33, 253–273.
Hanlon, F.M., Miller, G.A., Thoma, R.J., Irwin, J., Jones, A., Moses, S.N., et al., 2005. Distinct M50 and M100 auditory gating deficits in schizophrenia. Psychophysiology 42, 417–427.
Hirano, Y., Onitsuka, T., Kuroki, T., Matsuki, Y., Hirano, S., Maekawa, T., Kanba, S., 2008. Auditory sensory gating to the human voice: a preliminary MEG study. Psychiatry Res. 163, 260–269.
Hirano, Y., Hirano, S., Maekawa, T., Obayashi, C., Oribe, N., Monji, A., Kasai, K., Kanba, S., Onitsuka, T., 2010. Auditory gating deficit to human voices in schizophrenia: a MEG study. Schizophr. Res. 117, 61–67.
Jäncke, L., Hanggi, J., Steinmetz, H., 2004. Morphological brain differences between adult stutterers and non-stutterers. BMC Neurol. 4, 23.
Jessen, F., Kucharski, C., Fries, T., Papassotiropoulos, A., Hoenig, K., Maier, W., Heun, R., 2001. Sensory gating deficit expressed by a disturbed suppression of the P50 event-related potential in patients with Alzheimer's disease. Am. J. Psychiatry 158, 1319–1321.
Jones, M., Onslow, M., Harrison, E., Packman, A., 2000. Treating stuttering in young children: predicting treatment time in the Lidcombe Program. J. Speech Hear. Res. 43, 1440–1450.
Jones, M., Onslow, M., Packman, A., Williams, S., Ormond, T., Schwarz, I., et al., 2005. Randomised controlled trial of the Lidcombe programme of early stuttering intervention. BMJ 331, 659–661.
Kalinowski, J., Armson, J., Roland-Mieszkowski, M., Stuart, A., Gracco, V.L., 1993. Effects of alterations in auditory feedback and speech rate on stuttering frequency. Lang. Speech 36, 1–16.
Kell, C.A., Neumann, K., von Kriegstein, K., Posenenske, C., von Gudenberg, A.W., Euler, H., Giraud, A.L., 2009. How the brain repairs stuttering. Brain 132, 2747–2760.
Knecht, S., Deppe, M., Drager, B., Bobe, L., Lohmann, H., Ringelstein, E., Henningsen, H., 2000. Language lateralization in healthy right-handers. Brain 123 (Pt 1), 74–81.
Korzyukov, O., Pflieger, M.E., Wagner, M., Bowyer, S.M., Rosburg, T., Sundaresan, K., Elger, C.E., Boutros, N.N., 2007. Generators of the intracranial P50 response in auditory sensory gating. Neuroimage 35, 814–826.
Lincoln, M., Packman, A., Onslow, M., 2006. Altered auditory feedback and the treatment of stuttering: a review. J. Fluency Disord. 31, 71–89.
Lu, B.Y., Edgar, J.C., Jones, A.P., Smith, A.K., Huang, M.X., Miller, G.A., Canive, J.M., 2007. Improved test–retest reliability of 50-ms paired-click auditory gating using magnetoencephalography source modeling. Psychophysiology 44, 86–90.
Lu, C., Peng, D., Chen, C., Ning, N., Ding, G., Li, K., Yang, Y., Lin, C., 2010. Altered effective connectivity and anomalous anatomy in the basal ganglia-thalamocortical circuit of stuttering speakers. Cortex 46, 49–67.
Månsson, H., 2000. Childhood stuttering incidence and development. J. Fluency Disord. 25, 47–57.
Max, L., Guenther, F.H., Gracco, V.L., Ghosh, S.S., Wallace, M.E., 2004. Unstable or Insufficiently Activated Internal models and feedback-biased motor control as sources of dysfluency: a theoretical model of stuttering. Contemp. Issues Commun. Sci. Disord. 31, 105–122.
Medvedovsky, M., Taulu, S., Bikmullina, R., Paetau, R., 2007. Artifact and head movement compensation in MEG. Neurol. Neurophysiol. Neurosci. 4, 1–10.
Mukamel, R., Gelbard, H., Arieli, A., Hasson, U., Fried, I., Malach, R., 2005. Coupling between neuronal firing, field potentials, and FMRI in human auditory cortex. Science 309, 951–954.
Naka, D., Kakigi, R., Hoshiyama, M., Yamasaki, H., Okusa, T., Koyama, S., 1999. Structure of the auditory evoked magnetic fields during sleep. Neuroscience 93, 573–583.
Neumann, K., Preibisch, C., Euler, H.A., von Gudenberg, A.W., Lanfermann, H., Gall, V., Giraud, A.L., 2005. Cortical plasticity associated with stuttering therapy. J. Fluency Disord. 30, 23–39.
Newman, P.W., Bunderson, K., Brey, R.H., 1985. Brain stem electrical responses of stutterers and normals by sex, ears, and recovery. J. Fluency Disord. 10, 59–67.
Oldfield, R.C., 1971. Assessment and analysis of handedness — Edinburgh inventory. Neuropsychologia 9, 97–113.
Onitsuka, T., Ninomiya, H., Sato, E., Yamamoto, T., Tashiro, N., 2000. The effect of interstimulus intervals and between-block rests on the auditory evoked potential and magnetic field: is the auditory P50 in humans an overlapping potential? Clin. Neurophysiol. 111, 237–245.
Özcan, Ö., Altınayar, S., Özcan, C., Ünal, S., Karlıdağ, R., 2009. P50 sensory gating in children and adolescents with developmental stuttering. Bull. Clin. Psychopharmacol. 19, 241–246.
Pantev, C., Lutkenhoner, B., Hoke, M., Lehnertz, K., 1986. Comparison between simultaneously recorded auditory-evoked magnetic fields and potentials elicited by ipsilateral, contralateral and binaural tone burst stimulation. Audiology 25, 54–61.
Pantev, C., Hoke, M., Lutkenhoner, B., Lehnertz, K., 1989. Tonotopic organization of the auditory-cortex — pitch versus frequency representation. Science 246, 486–488.
Pantev, C., Bertrand, O., Eulitz, C., Verkindt, C., Hampson, S., Schuierer, G., Elbert, T., 1995. Specific tonotopic organizations of different areas of the human auditory-cortex revealed by simultaneous magnetic and electric recordings. Electroencephalogr. Clin. Neurophysiol. 94, 26–40.
Pantev, C., Oostenveld, R., Engelien, A., Ross, B., Roberts, L.E., Hoke, M., 1998a. Increased auditory cortical representation in musicians. Nature 392, 811–814.
Pantev, C., Ross, B., Berg, P., Elbert, T., Rockstroh, B., 1998b. Study of the human auditory cortices using a whole-head magnetometer: left vs. right hemisphere and ipsilateral vs. contralateral stimulation. Audiol. Neurootol. 3, 183–190.
Pantev, C., Roberts, L.E, Schulz, M., Engelien, A., Ross, B., 2001. Timbre-specific enhancement of auditory cortical representations in musicians. Neuroreport 12, 169–174.
Postma, A., 2000. Detection of errors during speech production: a review of speech monitoring models. Cognition 77, 97–132.
Postma, A., Kolk, H., 1992. Error monitoring in people who stutter: evidence against auditory feedback defect theories. J. Speech Hear. Res. 35, 1024–1032.
Postma, A., Kolk, H., 1993. The covert repair hypothesis: prearticulatory repair processes in normal and stuttered disfluencies. J. Speech Hear. Res. 36, 472–487.
Rojas, D.C., Bawn, S.D., Carlson, J.P., Arciniegas, D.B., Teale, P.D., Reite, M.L., 2002. Alterations in tonotopy and auditory cerebral asymmetry in schizophrenia. Biol. Psychiatry 52, 32–39.
Salmelin, R., Schnitzler, A., Schmitz, F., Jancke, L., Witte, O.W., Freund, H.J., 1998. Functional organization of the auditory cortex is different in stutterers and fluent speakers. NeuroReport 9, 2225–2229.
Schaechter, J.D., Moore, C.I., Connell, B.D., Rosen, B.R., Dijkhuizen, R.M., 2006. Structural and functional plasticity in the somatosensory cortex of chronic stroke patients. Brain 129, 2722–2733.
Sommer, M., Koch, M.A., Paulus, W., Weiller, C., Buchel, C., 2002. Disconnection of speech-relevant brain areas in persistent developmental stuttering. Lancet 360, 380–383.
Stager, S.V., 1990. Heterogeneity in stuttering: results from auditory brainstem response testing. J. Fluency Disord. 15, 9–19.
Taulu, S., Simola, J., Kajola, M., 2004. MEG recordings of DC fields using the signal space separation method (SSS). Neurol. Clin. Neurophysiol. 35, 1–4.
Taulu, S., Simola, J., Kajola, M., 2005. Applications of the signal space separation method. IEEE Trans. Signal Process. 53, 3359–3372.
Thoma, R.J., Hanlon, F.M., Moses, S.N., Edgar, J.C., Huang, M., Weisend, M.P., Irwin, J., Sherwood, A., Paulson, K., Bustillo, J., et al., 2003. Lateralization of auditory sensory gating and neuropsychological dysfunction in schizophrenia. Am. J. Psychiatry 160, 1595–1605.
Thoma, R.J., Hanlon, F.M., Sanchez, N., Weisend, M.P., Huang, M., Jones, A., Miller, G.A., Canive, J.M., 2004. Auditory sensory gating deficit and cortical thickness in schizophrenia. Neurol. Clin. Neurophysiol. 62, 1–7.
Thoma, R.J., Hanlon, F.M., Petropoulos, H., Miller, G.A., Moses, S.N., Smith, A., Parks, L., Lundy, S.L., Sanchez, N.M., Jones, A., et al., 2008. Schizophrenia diagnosis and anterior hippocampal volume make separate contributions to sensory gating. Psychophysiology 45, 926–935.
Watkins, K.E., Smith, S.M., Davis, S., Howell, P., 2008. Structural and functional abnormalities of the motor system in developmental stuttering. Brain 131, 50–59.
Weiland, B.J., Boutros, N.N., Moran, J.M., Tepley, N., Bowyer, S.M., 2008. Evidence for a frontal cortex role in both auditory and somatosensory habituation: a MEG study. Neuroimage 42, 827–835.
Weisser, R., Weisbrod, M., Roehrig, M., Rupp, A., Schroeder, J., Scherg, M., 2001. Is frontal lobe involved in the generation of auditory evoked P50? NeuroReport 12, 3303–3307.

Clinical Neurophysiology 122 (2011) 777–783

Contents lists available at ScienceDirect

Clinical Neurophysiology

journal homepage: www.elsevier.com/locate/clinph

# Transcranial direct current stimulation over the motor association cortex induces plastic changes in ipsilateral primary motor and somatosensory cortices

Hikari Kirimoto [a,*], Katsuya Ogata [c,1], Hideaki Onishi [b], Mineo Oyama [a], Yoshinobu Goto [d], Shozo Tobimatsu [c]

[a] Department of Occupational Therapy, Faculty of Rehabilitation, Niigata University of Health and Welfare, Japan
[b] Department of Physical Therapy, Faculty of Rehabilitation, Niigata University of Health and Welfare, Japan
[c] Department of Clinical Neurophysiology, Neurological Institute, Faculty of Medicine, Graduate School of Medical Sciences, Kyushu University, Japan
[d] Department of Occupational Therapy, Faculty of Rehabilitation, International University of Health and Welfare, Japan

See Editorial, pages 643–644

ARTICLE INFO

*Article history:*
Accepted 4 September 2010
Available online 11 November 2010

*Keywords:*
Transcranial direct current stimulation
Premotor cortex
Motor evoked potentials
Somatosensory evoked potentials
Plasticity

ABSTRACT

*Objective:* This study was performed to elucidate whether transcranial direct current stimulation (tDCS) over the motor association cortex modifies the excitability of primary motor (M1) and somatosensory (S1) cortices via neuronal connectivity.
*Methods:* Anodal, cathodal, and sham tDCS (1 mA) over the left motor association cortex was applied to 10 subjects for 15 min using electrodes of two sizes (9 and 18 $cm^2$). Both motor evoked potentials (MEPs) and somatosensory evoked potentials (SEPs) were recorded before, immediately after, and 15 min after tDCS. Electrode positions were confirmed by overlaying them on MRI anatomical surface images of two individuals.
*Results:* After applying anodal tDCS using the large electrode, amplitudes of MEP components significantly decreased, whereas those of early SEP components (N20 and P25) increase. Opposite effects were observed on MEPs and SEPs after cathodal tDCS. However, a small electrode did not significantly influence either MEPs or SEPs, irrespective of polarity. The small electrode covered mainly the dorsal premotor cortex (PMd) while the large electrode involved the supplementary motor area (SMA) in addition to PMd.
*Conclusions:* These results suggest that anodal tDCS over PMd together with SMA enhanced the inhibitory input to M1 and excitatory input to S1, and that cathodal tDCS might lead to an opposite effect.
*Significance:* The finding that only the large electrode modulated M1 and S1 implies that activation of PMd together with SMA by tDCS can induce plastic changes in primary sensorimotor areas.


## 1. Introduction

Nitsche and Paulus (2000) first described the efficacy of transcranial direct current stimulation (tDCS) for functional modulation of the human motor cortex. Since then, tDCS has become an increasingly useful technique for noninvasive brain stimulation that can be used not only to examine cortical function in healthy subjects but also to facilitate the treatment of various neurological disorders (Schlaug et al., 2008).

During tDCS, electrodes are placed and secured to the scalp over the desired areas and currents are delivered to the underlying cortical tissue. The direction of current flow determines the effects on the underlying tissue. When tDCS is applied over the primary motor cortex (M1), anodal tDCS (using the anodal electrode over M1 and the cathodal electrode over the contralateral orbit) enhances cortical excitability, which increases the amplitude of motor evoked potentials (MEPs). On the other hand, cathodal tDCS (using the cathodal electrode over M1) shows the opposite effect (Nitsche and Paulus, 2000).

In addition to studies of the direct functional effects of tDCS over M1 (Nitsche and Paulus, 2000; Nitsche et al., 2003a, 2007;

* Corresponding author at: Department of Occupational Therapy, Faculty of Rehabilitation, Niigata University of Health and Welfare, 1398 Shimami-cho, Kita-ku, Niigata 950-3198, Japan. Tel./fax: +81 25 257 4737.
*E-mail address:* kirimoto@nuhw.ac.jp (H. Kirimoto).
[1] Equal contribution to this study.

1388-2457/$36.00 
doi:10.1016/j.clinph.2010.09.025

Hummel et al., in press; Stagg et al., 2009) and the primary sensory cortex (S1) (Matsunaga et al., 2004; Dieckhöfer et al., 2006), which were spatially restricted, remote effects were observed after motor cortex–prefrontal tDCS in a positron emission tomography (PET) study (Lang et al., 2005). A recent study also reported that anodal tDCS over the premotor cortex (PM) reduced short-interval intracortical inhibition (SICI) at interstimulus interval (ISI) of 2 and 3 ms, and enhanced intracortical facilitation (ICF) at ISI of 10 and 15 ms and the MEP amplitude of ISI of 7 ms, while motor thresholds, single test-pulse MEPs, and input–output curves of MEPs remained unchanged (Boros et al., 2008). However, cathodal tDCS had no remarkable effect.

In repetitive transcranial magnetic stimulation (rTMS) studies, low-frequency rTMS (1 Hz) at 90% active motor threshold (AMT) over PM caused a long-lasting reduction in M1 excitability measured by single-pulse TMS (Gerschlager et al., 2001; Rizzo et al., 2003). In contrast, rTMS of 1 Hz at 80% AMT over PM had no after-effects on single test-pulse MEP but significantly facilitated ICI (Münchau et al., 2002). Interestingly, high-frequency rTMS (5 Hz) at 90% AMT resulted in the increase of M1 excitability with decreased ICI and vice versa at 80% AMT (Rizzo et al., 2003). Thus, the intensity and frequency of rTMS are important to induce up- or down-regulation of the excitability in distinct neuronal circuits of M1. However, the mechanism of remote effect by tDCS has not been fully elucidated. It is possible that rTMS and tDCS could share the mechanism of the modification of neuronal connectivity. Therefore, we examined the possibility that tDCS over PM modulates the functions of S1 and M1 in a manner similar to rTMS over PM which changes S1 excitability (Hosono et al., 2008). PM is specialized for the control of externally triggered motor actions (Mushiake et al., 1991) and is activated more strongly by symbolic cues (Schluter et al., 1998) and codes for hand and eye position (Pesaran et al., 2006). Our previous functional MRI study demonstrated that a significant relationship exists between PM and the sensorimotor cortex during externally guided movements (Tanizaki et al., 2003). However, the neuronal connectivity of PM–M1–S1 has not yet been directly evaluated. The aim of this study was therefore, to determine whether tDCS over PM modifies the excitability of ipsilateral M1 and S1 via cortico-cortical connectivity.

## 2. Methods

### 2.1. Subjects

Ten healthy college students (7 males, 3 females; mean age, 20.6 years; range, 20–21 years) participated in this study. None of them had received medical treatment for any condition. Informed consent was obtained before beginning the experiment, which was conducted according to the Declaration of Helsinki. The experimental procedures were also approved by the Ethics Committee of the Niigata University of Health and Welfare.

### 2.2. Experimental procedures

During the experiment, subjects were seated on a comfortable reclining armchair with a mounted headrest. All experimental protocols were performed in the neutral forearm position. To avoid carryover effects, all subjects participated in three experimental sessions on separate days that were at least a week apart. All subjects received cathodal, anodal, or sham tDCS (1 mA) using a large ($4 \times 4.5$ cm; 18 $cm^2$) electrode over the left PM for 15 min in a counterbalanced order. As an additional experiment, tDCS over PM using a small ($3 \times 3$ cm; 9 $cm^2$) electrode was performed in 6 of the 10 subjects. Because we performed this experiment to determine whether MEPs and somatosensory evoked potentials (SEPs) would change in a manner similar to that observed using the large electrode, we eliminated the sham condition in the experiment performed using the small electrode, and the subjects received only anodal and cathodal tDCS. MEPs from the right first dorsal interosseus (FDI) muscle with TMS over the left M1 and SEPs following right median nerve stimulation were recorded from the left C3′ (2 cm posterior to C3 of the International 10–20 system) before, immediately after, and 15 min after tDCS.

### 2.3. tDCS over the motor association cortex

In several previous rTMS studies, the stimulation site over PM was 2 cm anterior and 1 cm medial to the motor hotspot. This area was estimated as the dorsal PM (PMd) in a PET study (Fink et al., 1997). If the "conventional electrode ($7 \times 5$ cm)" (Nitsche et al., 2007) is centered 2 cm anterior and 1 cm medial to the motor hotspot, the covered area could overlap the motor hotspot and cross the vertex. Therefore, the electrode size was reduced to 18 or 9 $cm^2$ in this study. The large electrode ($4 \times 4.5$ cm = 18 $cm^2$) was centered 2 cm anterior and 3 cm medial to the motor hotspot, while the small electrode ($3 \times 3$ cm = 9 $cm^2$) was centered 2 cm anterior and 1 cm medial to avoid covering the motor hotspot with the edge of the electrode (Fig. 1).

Conductive thick (0.3 cm) rubber rectangular electrodes covered with a saline-soaked sponge were placed on the scalp over the left PM. The reference electrode ($4 \times 4.5$ cm = 18 $cm^2$) was placed on the contralateral forehead above the orbit. The scalp around PM was cleaned with alcohol, and electrode paste (Gelaid, Nihon Koden, Japan) was applied to reduce electrode impedance. Stimuli were applied using a constant current electrical stimulator (Eldith, NeuroConn GmbH, Germany).

Current strength was set at 1 mA for the large electrode but reduced to 0.5 mA for the small electrode to keep the current density constant (0.055 mA/$cm^2$). During stimulation, the DC current was initially increased in a ramp-like manner at 10-s intervals until current strength of 1 mA or 0.5 mA was obtained (Gandiga et al., 2006). tDCS was maintained for a total of 15 min. In sham experiments, tDCS was turned off after 30 s. The parameters for sham stimulation were derived from a previous report (Gandiga et al., 2006) in which perceived sensations on the skin, such as tingling, usually faded out during the first 30 s of tDCS. Under both conditions, the DC current was slowly turned off over the course of 10 s, out of the subject's view. This procedure did not elicit any perceived sensations. The session order was counterbalanced and subjects were blinded to tDCS conditions.

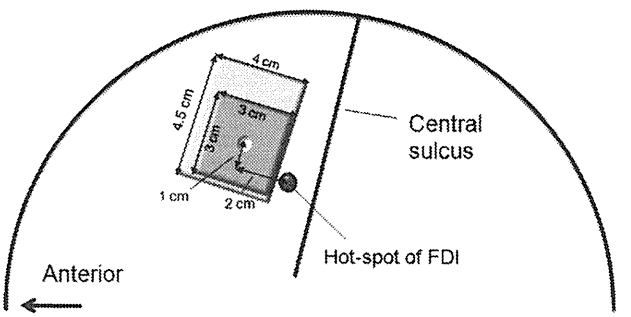


**Fig. 1.** Schematic illustration of the stimulus site over PM. The large electrode ($4 \times 4.5$ cm = 18 $cm^2$) was centered 2 cm anterior and 3 cm medial to the motor hotspot, while the small electrode ($3 \times 3$ cm = 9 $cm^2$) was centered 2 cm anterior and 1 cm medial to avoid covering the motor hotspot with the edge of the electrode. The reference electrode ($4 \times 4.5$ cm = 18 $cm^2$) was placed on the contralateral forehead above the orbit.

To prevent the subject from feeling pain, Nitsche et al. (2003b) recommended that current density should not exceed 0.02857 mA/cm$^2$. The current density used in this experiment (0.055 mA/cm$^2$) was higher than the recommended value. However, the current density in our study is comparable to that (0.05–0.057 mA/cm$^2$) used in previous studies in which side effects or pain sensation was not observed (Jeffery et al., 2007; Tanaka et al., 2009; Roche et al., 2010).

Exact stimulating electrode positions over the cortex were evaluated in 2 of the 10 subjects. Standard T1-weighted images were obtained (Signa HDi 1.5 T; GE Healthcare, Japan; 1.5 T, 1-mm slice), and electrode positions were confirmed by overlaying them on MRI anatomical surface images of each individual using a 3D magnetic space digitizer (Fastrak; Polhemus, USA) and specific software (Fusion; Shimazu Co. Ltd., Japan) (Maki et al., 1995; Okamoto et al., 2006; Shibusawa et al., 2009).

### 2.4. MEP recordings

MEPs elicited by TMS were recorded from the right FDI muscle. TMS was performed using a standard double (figure-of-eight) 70-mm coil connected to a monophasic Magstim 200 stimulator (Magstim, UK). The coil was placed tangentially to the scalp with the handle pointing posterolaterally 45 degrees from the midline. We determined the optimal position for activation of the right FDI muscle by moving the coil around the presumed hand motor area in M1 (approximately 4–6 cm lateral and 2 cm anterior to the vertex). The site at which TMS of slightly suprathreshold intensity consistently elicited the largest MEP in the FDI muscle was marked as the motor hotspot. The output of the stimulator was set to obtain an MEP of amplitude 1–1.5 mV (10% of M max) in the relaxed FDI muscle (Todd et al., 2006). TMS was delivered 12 times at 0.2 Hz with the subjects being asked to keep the muscle relaxed. Complete muscle relaxation was confirmed online via audiovisual feedback of electromyographic (EMG) activity.

Surface EMG was recorded using disposable silver–silver chloride surface electrodes. Recording and reference electrodes were placed over the muscle and the tendon. EMG signals were amplified (100×) and bandpass filtered (5–500 Hz) using a preamplification system (DL-140; 4 Assist, Japan) and digitized at 10 kHz (PowerLab; AD Instruments, Australia). Data were recorded and stored for off-line analysis (Scope; AD Instruments) on a personal computer.

### 2.5. SEP recordings

SEPs were recorded from the left parietal area during right median nerve stimulation at the wrist. A recording electrode was placed 2 cm posterior to C3 of the International 10–20 system. A reference electrode was placed on the right earlobe. SEPs were amplified with bandpass filters set at 0.2–1000 Hz and 300 responses were averaged. Brief electrical stimulation (0.2 ms) was delivered to the right median nerve at a frequency of 3 Hz (Neuropack Σ; Nihon Kohden, Japan). The stimulus intensity was fixed at about 1.2 times the motor threshold. SEP data were stored and analyzed using the same computer systems as those used for MEPs.

### 2.6. Data and statistical analysis

Peak-to-peak amplitudes of MEPs were measured after excluding trials with excessive artifacts. Mean MEP amplitudes were calculated from at least 8 of the 12 trials. Peak-to-peak amplitudes of four cortical SEP components, i.e., N20, P25, N33, and P45, were also analyzed. The amplitude of each component was measured from the preceding peaks.

Amplitudes of MEPs and SEPs were normalized to those recorded before tDCS. All data were expressed as means ± SEM and were statistically analyzed by two-way repeated measures analysis of variance (ANOVA) with the parameters polarity of tDCS (anodal vs. cathodal vs. sham) and time (before vs. immediately after vs. 15 min after). The sphericity of the data was tested by the Mauchly's test, and Greenhouse–Geisser corrected significance values were used when sphericity was lacking. Post hoc analysis was performed with Bonferroni's correction for multiple comparisons. A difference was accepted as significant at $p < 0.05$ for all analyses.

## 3. Results

### 3.1. MEPs after tDCS over the motor association cortex

Fig. 2 shows MEP waveforms recorded from a representative subject before, immediately after, and 15 min after anodal and cathodal tDCS over PM under the large electrode (18 cm$^2$) condition. The MEP amplitudes before tDCS in each stimulus condition were comparable: anodal 0.96 ± 0.06 mV, cathodal 0.94 ± 0.07 mV and sham 1.06 ± 0.07 mV, respectively. MEP amplitudes after anodal tDCS using the large electrode decreased markedly, whereas those after cathodal tDCS increased significantly. However, tDCS using the small electrode (9 cm$^2$) showed no remarkable effect.

Under the large electrode condition, two-way repeated measures ANOVA revealed a significant main effect of polarity of tDCS ($F_{1.92,\ 17.24} = 6.232$, $p = 0.01$) and interaction between polarity of tDCS and time ($F_{2.23,\ 20.69} = 8.211$, $p = 0.002$), but no significant main effect of time was observed. Post hoc analysis showed a significant difference between anodal and cathodal tDCS at both immediately after ($p < 0.001$) and 15 min after ($p = 0.027$) stimulation, and also between anodal and sham tDCS at immediately after

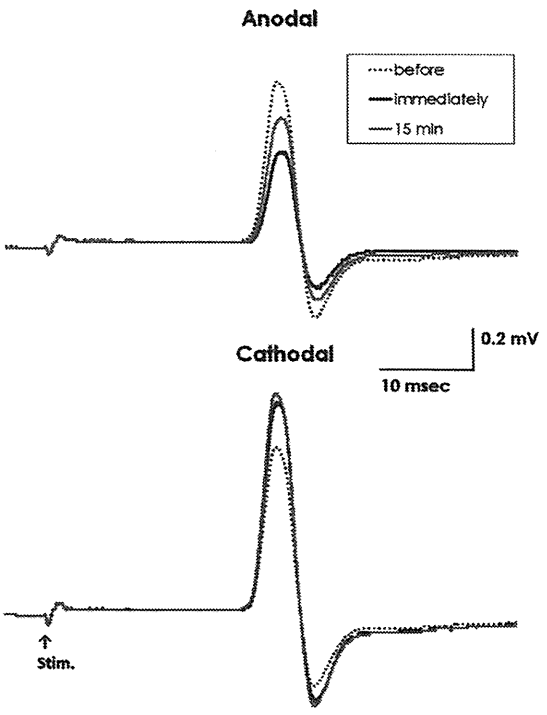


**Fig. 2.** MEP waveforms with TMS over M1 recorded from a representative subject before, immediately after, and 15 min after anodal and cathodal tDCS over the motor association cortex. The dotted lines represent MEPs prior to tDCS, black lines represent MEPs immediately after tDCS, and gray lines represent MEPs 15 min after tDCS. MEP amplitudes after anodal tDCS over the motor association cortex decreased, whereas those after cathodal tDCS increased.

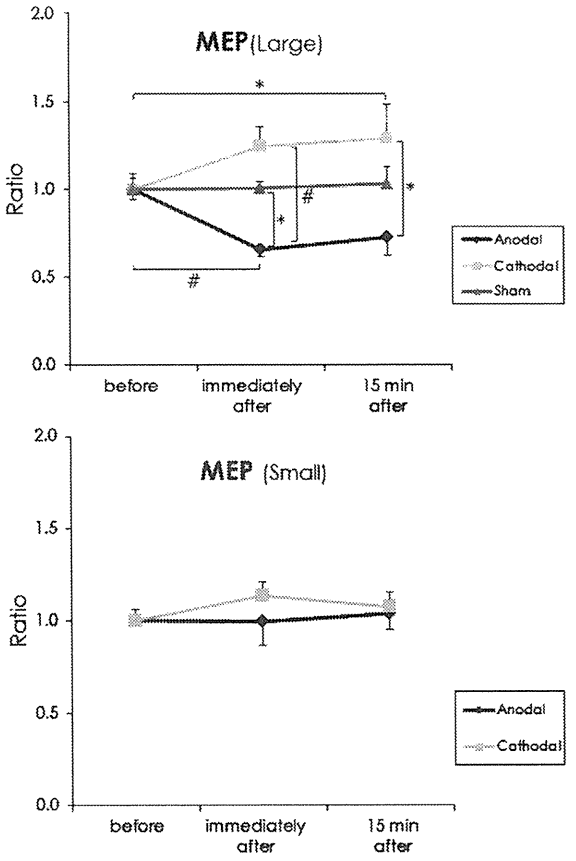


**Fig. 3.** Serial changes in MEP amplitudes before, immediately after, and 15 min after anodal, cathodal and sham tDCS under the large electrode condition (above), and anodal and cathodal tDCS under the small electrode condition (below). MEP amplitudes decreased markedly after anodal tDCS using the large electrode, whereas those after cathodal tDCS increased significantly. However, tDCS using the small electrode showed no remarkable effect. MEP amplitudes are normalized to those recorded before tDCS (mean ± SEM). ($^{*}p < 0.05$; $^{\#}p < 0.01$).

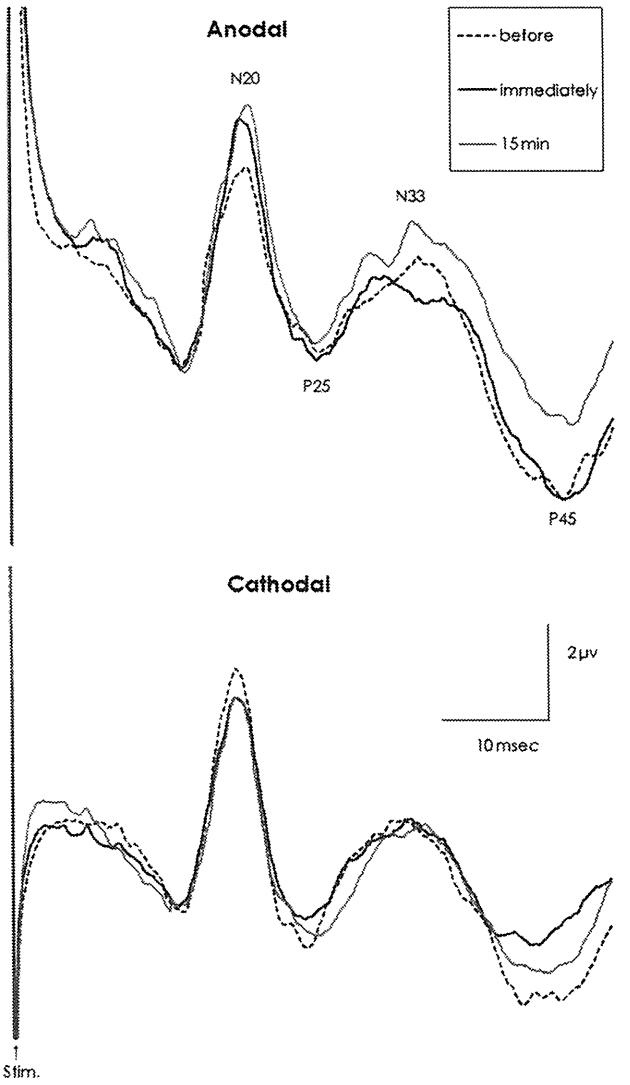


**Fig. 4.** SEP waveforms recorded from the left parietal area after right median nerve stimulation in a representative subject before, immediately after, and 15 min after anodal and cathodal tDCS over the motor association cortex. The dotted lines represent SEPs prior to tDCS, black lines represent SEPs immediately after tDCS, and gray lines represent SEPs 15 min after tDCS. SEP amplitudes increased after anodal tDCS but decreased after cathodal tDCS.

stimulation ($p = 0.035$). A significant difference between before and 15 min after stimulation was observed for anodal tDCS ($p = 0.038$) as well as between before and immediately after stimulation for cathodal tDCS ($p < 0.001$). In contrast, no significant main effect or interaction was observed under the small electrode condition (Fig. 3).

### 3.2. SEPs after tDCS over the motor association cortex

Fig. 4 shows SEP waveforms recorded from a representative subject before, immediately after, and 15 min after anodal and cathodal tDCS over PM under the large electrode condition. The amplitudes of N20 and P25 before tDCS in each stimulus condition were comparable: N20, anodal 3.37 ± 0.24 μV, cathodal 3.20 ± 0.23 μV and sham 3.62 ± 0.43 μV; P25, anodal 3.06 ± 0.34 μV, cathodal 3.22 ± 0.13 μV and sham 2.94 ± 0.09 μV, respectively. Contrary to the results obtained for MEPs, SEP amplitudes of N20 and P25 after anodal tDCS using the large electrode tended to increase, while those after cathodal tDCS decreased. However, tDCS using the small electrode showed no comparable effect.

Under the large electrode condition, two-way repeated measures ANOVA revealed a significant main effect of polarity ($F_{1.67,\ 15.02} = 11.702$, $p < 0.001$) and interaction between polarity and time ($F_{2.23,\ 20.11} = 3.819$, $p = 0.011$) for the N20 component. Post hoc analysis showed a significant difference between anodal and cathodal tDCS at both immediately after ($p = 0.013$) and 15 min after ($p = 0.01$) stimulation, between anodal and sham tDCS 15 min after stimulation ($p = 0.015$) and between cathodal and sham immediately after stimulation ($p = 0.024$). There was a significant main effect of polarity ($F_{1.12,\ 10.12} = 13.238$, $p < 0.001$) for the P25 component, but no main effect of time or interaction between polarity and time. Post hoc analysis revealed a significant difference between anodal and cathodal tDCS ($p < 0.001$), and between anodal and sham tDCS ($p = 0.013$) (Fig. 5). No significant effects of tDCS were observed for the N33 and P45 components. Under the small electrode condition, no significant main effect or interaction was observed for any component.

### 3.3. Stimulus sites

The position of the tDCS electrode was evaluated using a three-dimensional (3D) image (Fig. 6). Both large and small electrodes covered mainly PMd (Rizzolatti and Arbib, 1998; Bäumer et al., 2009) and a portion of the anterior part of PM (Civardi et al., 2001), but the large electrode further involved the supplementary

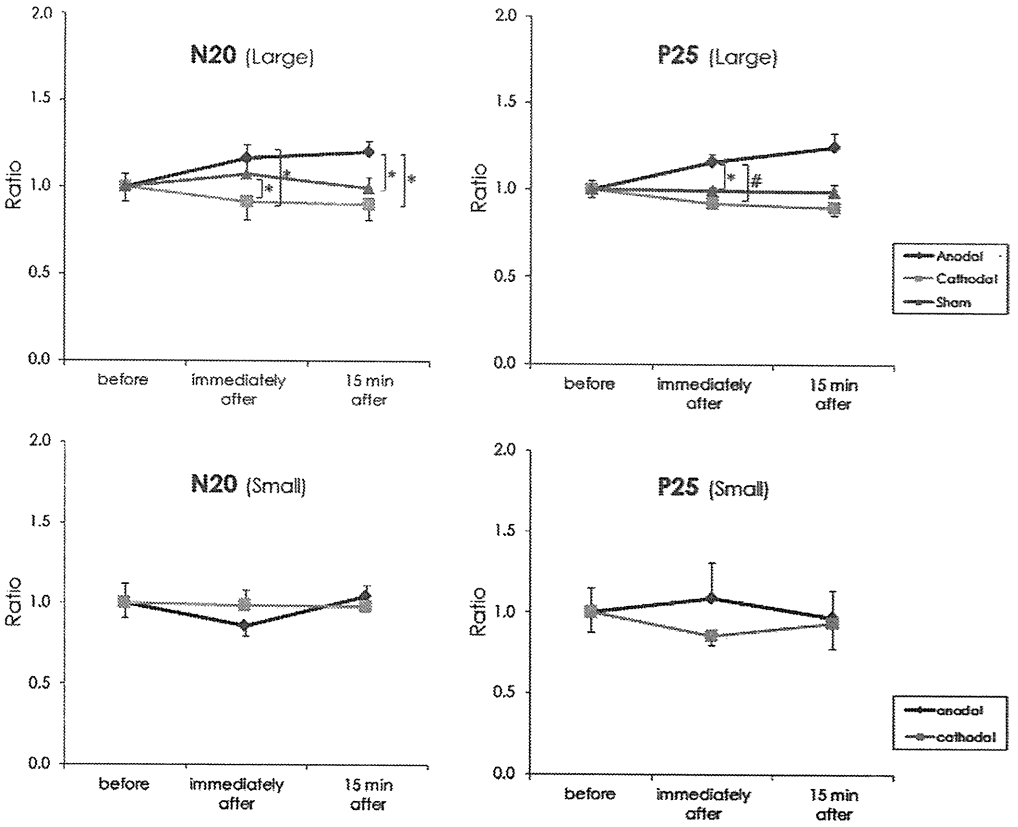


**Fig. 5.** Serial changes in SEP amplitudes (N20 and P25) before, immediately after, and 15 min after anodal, cathodal and sham tDCS under the large electrode condition (above), and anodal and cathodal tDCS under the small electrode condition (below). Contrary to the results for MEPs, N20 and P25 amplitudes after anodal tDCS using the large electrode increased compared with the cathodal condition, whereas those after cathodal tDCS decreased. However, tDCS using the small electrode showed no significant effect. SEP amplitudes are normalized to those recorded before tDCS (mean ± SEM). ($^{*}p < 0.05$; $^{\#}p < 0.01$).

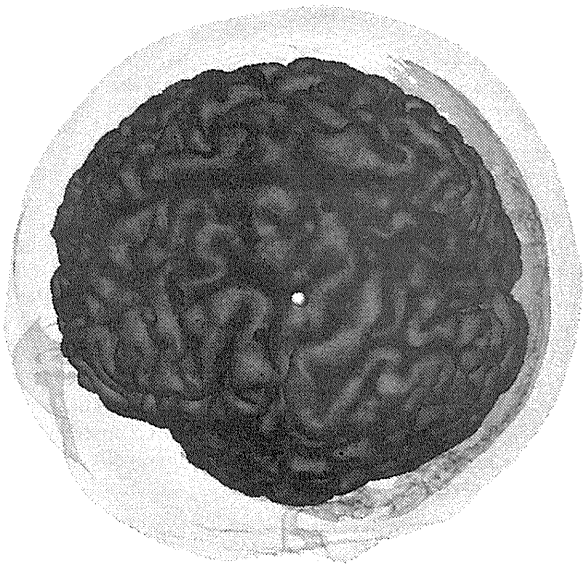

**Fig. 6.** tDCS electrode positions overlaid on MRI surface images. Edges of the electrodes are shown by red dots for the small electrode and blue dots for the large electrode. The white dot indicates the motor hotspot of FDI. Both the large and small electrodes covered mainly PMd and a portion of the anterior part of PM, while the large electrode also covered the supplementary motor area (SMA) but did not reach PMv and the contralateral hemisphere.

motor area (SMA) without reaching ventral PM (PMv) or the contralateral hemisphere.

## 4. Discussion

This study demonstrated that tDCS over the motor association cortex using the large electrode modulated the excitability of ipsilateral M1 and S1. Interestingly, this manipulation induced opposite effects on M1 and S1. After anodal tDCS, amplitudes of MEPs significantly decreased compared with cathodal condition, whereas those of early SEP components (N20 and P25) increased. In contrast, the amplitudes of MEPs and SEPs did not show overt changes in the sham condition. Since the significant differences were observed between anodal/cathodal and sham conditions, the changes in M1 and S1 excitability can be caused by direct tDCS effect but not by changes in attention, habituation and fatigue resulted from repetitive measurements. Therefore, our result suggests that M1 was inhibited whereas S1 was excited by activation of PM and SMA after anodal tDCS. Opposite effects were observed after cathodal tDCS. However, the small electrode, which covered PMd but not SMA, did not significantly affect M1 or S1, irrespective of the polarity. Therefore, simultaneous modulation of PMd and SMA may alter the function of the sensorimotor network.

### *4.1. Changes in M1 excitability after tDCS over the motor association cortex*

Nitsche and Paulus (2000) showed that anodal tDCS induced an excitatory effect, whereas cathodal tDCS produced an inhibitory ef-

fect over the cortex. In our study, presumed excitatory stimulation (anodal) over PMd and SMA reduced the MEP size, and inhibitory cathodal stimulation showed the opposite effect. Therefore, anodal tDCS activated the inhibitory connection to M1 whereas cathodal tDCS inhibited this connection, which in turn disinhibited M1.

Current density (current intensity/electrode size), duration, polarity, and location of stimulation have important implications in the neuromodulatory outcome (Zaghi et al., 2010). Nitsche et al. (2007) reported that the effect of tDCS did not diminish if the current density was held constant even when the size of the stimulation electrode and current strength were reduced. In this study, the current strength was set at 1 mA for the large electrode and was reduced to 0.5 mA for the small one to keep the current density constant (0.055 mA/cm$^2$). The effects on M1 excitability differed between the two electrodes. Thus, the difference in the area covered by tDCS is likely to cause the difference in the effects. tDCS electrodes of both sizes were evaluated by a 3D image and were found to cover PMd, but only the large electrode included SMA. We assume that tDCS over not only PMd but also SMA might be necessary to modulate the excitability of M1 and S1. Our results appear to differ from those of a recent tDCS study (Boros et al., 2008); anodal tDCS over PM decreased SICI and increased intracortical facilitation (ICF), whereas motor thresholds, single test-pulse MEPs, and input–output curves of MEPs remained stable in that study. However, our study findings are in part consistent with those of their study in that tDCS limited to PMd using the small electrode had no effect on single-pulse MEPs, although we did not evaluate SICI/ICF by paired-pulse TMS. Boros et al. (2008) used a large rectangular electrode (3 × 11 cm) to stimulate PM, and this large electrode may cover almost the entire PM area (PMd and PMv). This suggests that tDCS over PM using a large electrode could selectively modulate cortico-cortical excitability (SICI and ICF) but not corticospinal excitability (single-pulse MEPs and input–output curves). However, stimulating PMd as well as SMA would modulate corticospinal excitability as shown in our study.

High-frequency rTMS over PMd or SMA increased MEP amplitudes (Rizzo et al., 2003; Matsunaga et al., 2005; Raux et al., 2010). Conversely, low-frequency (1 Hz) rTMS decreased M1 excitability (Gerschlager et al., 2001; Münchau et al., 2002; Rizzo et al., 2003). However, Rizzo et al. (2003) demonstrated that high-frequency rTMS over PMd did not always increase M1 excitability. They found that 1- and 5-Hz rTMS over PMd had the opposite effect on ipsilateral M1 and that these effects alternated depending on the intensity of rTMS. Their results suggest that rTMS over PM can induce up- or down-regulation of neuronal circuits to M1 when a certain intensity and frequency are selected. Interestingly, Civardi et al. (2001) examined connections to M1 from frontal and medial cortices. Conditioning TMS 4–6 cm lateral to the motor hotspot reduced MEP amplitudes, whereas conditioning TMS 2 cm lateral increased these amplitudes. These results indicate that the motor association cortex has facilitatory and inhibitory neural connections to M1. Therefore, anodal tDCS over the motor association cortex using the large electrode might have increased mainly the inhibitory input to M1 in this study.

### 4.2. Possibility of current spread to M1

Nitsche et al. (2007) conducted a control experiment to rule out the possibility that tDCS-generated motor cortical excitability shifts were caused by transfer of current flow. They stimulated the hotspot of the abductor digiti minimi (ADM) with tDCS using a small electrode (3.5 cm$^2$) and showed selective enhancement of MEP amplitude after anodal tDCS of ADM but not FDI. This result suggests that tDCS-generated modulation of cortical excitability can be restricted to the area under the stimulation electrode.

Edges of both the small and large electrodes in the present study were close to, but did not cover, FDI hotspot. Moreover, our study showed the differential effects of the two sizes of electrode, even though these electrodes were similarly close to the hotspot. Thus, we conclude that the difference in the excitability of M1 and S1 was caused by the neuronal connectivity from the motor association cortex to the sensorimotor cortex and not merely by the transfer of current flow over the scalp.

### 4.3. Sensorimotor interaction by tDCS over the motor association cortex

SEPs of the parietal electrode in this study were enhanced by anodal tDCS compared with the cathodal condition when MEPs were inhibited, and the effect was opposite for cathodal tDCS. Thus, S1 excitability was modulated in the direction opposite to that of M1 excitability. Several studies of rTMS or tDCS over M1 suggested that the amplitudes of MEPs and SEPs did not change in the opposite direction (Enomoto et al., 2001; Tsuji and Rothwell, 2002; Matsunaga et al., 2004; Wolters et al., 2005; Dieckhöfer et al., 2006), except for a report which showed that inhibitory theta burst stimulation over M1 enhanced SEPs (Ishikawa et al., 2007). Alternatively, low-frequency or inhibitory rTMS over PM, which should inhibit MEPs as described in the previous section, increased SEP amplitudes (Hosono et al., 2008). The findings of Hosono et al. (2008) are compatible with those of our study in that S1 excitability is modulated in a direction opposite to that of M1 excitability. Thus, modulation of the motor association cortex might cause bidirectional modulation of MEPs and SEPs. We assume that these bidirectional modulations might be similar to mechanisms of SEP gating in which SEPs are inhibited when M1 is activated for movement. Parietal SEPs are known to be attenuated before spontaneous voluntary movement (Ogata et al., 2009) in which SMA as well as PMd can be important elements for sensorimotor circuits (Taniwaki et al., 2003). Anatomical and physiological studies in animals (Dum and Strick, 1991; Stepniewska et al., 2006) and in our fMRI study (Taniwaki et al., 2003) have shown neuronal connections between M1/S1 and PM/SMA. Abnormal sensory processing in the hand before movement has been reported in cases of dystonia (Murase et al., 2000; Kaji et al., 2005) in which PM hyperactivity during writing was reported in a study using $H_2{}^{15}O$ PET (Ceballos-Baumann et al., 1997). Taken together, these results indicate that a functional connectivity might exist between PM/SMA and S1 via direct cortico-cortical connections or via indirect intercortical pathways such as M1.

In conclusion, anodal tDCS over the motor association cortex decreased MEP and increased SEP amplitudes compared with cathodal tDCS, which would result from increases in inhibitory inputs from PM/SMA to M1 and from excitatory inputs to S1 and vice versa for cathodal tDCS. Therefore, tDCS is useful for modulating PM/SMA excitability and assessing the plastic functions of M1 and S1.

## Acknowledgments

This work was supported in part by a Grant-in-Aid for Scientific Research (C) No. 08042773 from the Japan Society for the Promotion of Science and a research grant from Niigata University of Health and Welfare.

## References

Bäumer T, Schippling S, Kroeger J, Zittel S, Koch G, Thomalla G, et al. Inhibitory and facilitatory connectivity from ventral premotor to primary motor cortex in healthy humans at rest-A bifocal TMS study. Clin Neurophysiol 2009;120:1724–31.

Boros K, Poreisz C, Münchau A, Paulus W, Nitsche MA. Premotor transcranial direct current stimulation (tDCS) affects primary motor excitability in humans. Eur J Neurosci 2008;27:1292–300.
Ceballos-Baumann AO, Sheean G, Passingham RE, Marsden CD, Brooks DJ. Botulinum toxin does not reverse the cortical dysfunction associated with writer's cramp. A PET study. Brain 1997;120:571–82.
Civardi C, Cantello R, Asselman P, Rothwell JC. Transcranial magnetic stimulation can be used to test connections to primary motor areas from frontal and medial cortex in humans. Neuroimage 2001;14:1444–53.
Dieckhöfer A, Waberski TD, Nitsche M, Paulus W, Buchner H, Gobbele H. Transcranial direct current stimulation applied over the somatosensory cortex – differential effect on low and high frequency SEPs. Clin Neurophysiol 2006;117:2221–7.
Dum RP, Strick PL. The origin of corticospinal projections from the premotor areas in the frontal lobe. J Neurosci 1991;11:667–89.
Enomoto H, Ugawa Y, Hnanajima K, Yuasa K, Mochizuki H, Terao Y, et al. Decreased sensory cortical excitability after 1 Hz rTMS over the ipsilateral primary motor cortex. Clin Neurophysiol 2001;112:2154–8.
Fink GR, Frackowiak RS, Pietrzyk U, Passingham RE. Multiple non-primary motor areas in the human cortex. J Neurophysiol 1997;77:2164–74.
Gandiga PC, Hummel FC, Cohen LG. Transcranial DC stimulation (tDCS): a tool for double-blind sham-controlled clinical studies in brain stimulation. Clin Neurophysiol 2006;117:845–50.
Gerschlager W, Siebner HR, Rothwell JC. Decreased corticospinal excitability after subthreshold 1 Hz rTMS over lateral premotor cortex. Neurology 2001;57:379–80.
Hosono Y, Urushihara R, Harada M, Murase N, Kunikane Y, Shimazu H, et al. Comparison of monophasic versus biphasic stimulation in rTMS over premotor cortex: SEP and SPECT studies. Clin Neurophysiol 2008;119:2538–45.
Hummel FC, Heise K, Celnik P, Floel A, Gerloff C, Cohen LG. Facilitating skilled right hand motor function in older subjects by anodal polarization over the left primary motor cortex. Neurobiol Aging, in press.
Ishikawa S, Matsunaga K, Nakanishi R, Kawahira K, Murayama N, Tsuji S, et al. Effect of theta burst stimulation over the human sensorimotor cortex on motor and somatosensory evoked potentials. Clin Neurophysiol 2007;118:1033–43.
Jeffery DT, Norton JA, Roy FD, Gorassini MA. Effects of transcranial direct current stimulation on the excitability of the leg motor cortex. Exp Brain Res 2007;182:281–7.
Kaji R, Urushihara R, Murase N, Shimazu H, Goto S. Abnormal sensory gating in basal ganglia disorders. J Neurol 2005;252:13–6.
Lang N, Siebner HR, Ward NS, Lee L, Nitsche MA, Paulus W, et al. How does transcranial DC stimulation of the primary motor cortex alter regional neuronal activity in the human brain? Eur J Neurosci 2005;22:495–504.
Maki A, Yamashita Y, Ito Y, Watanabe E, Mayanagi Y, Koizumi H. Spatial and temporal analysis of human motor activity using noninvasive NIR topography. Med Phys 1995;22:1997–2005.
Matsunaga K, Nitsche MA, Tsuji S, Rothwell JC. Effect of transcranial DC sensorimotor cortex stimulation on somatosensory evoked potentials in humans. Clin Neurophysiol 2004;115:456–60.
Matsunaga K, Maruyama A, Fujiwara T, Nakanishi R, Tsuji S, Rothwell JC. Increased corticospianal excitability after 5 Hz rTMS over the human supplementary motor area. J Physiol (Lond) 2005;562:295–306.
Münchau A, Bloem BR, Irlbacher K, Trimble MR, Rothwell JC. Functional connectivity of human premotor and motor cortex explored with repetitive transcranial magnetic stimulation. J Neurosci 2002;22:554–61.
Murase N, Kaji R, Shimazu H, Katayama-Hirota M, Ikeda A, Kohara N, et al. Abnormal premovement gating of somatosensory input in writer's cramp. Brain 2000;123:1813–29.
Mushiake H, Inase M, Tanji J. Neuronal activity in the primate premotor, supplementary, and precentral motor cortex during visually guided and internally determined sequential movements. J Neurophysiol 1991;66: 705–18.
Nitsche MA, Paulus W. Excitability changes induced in the human motor cortex by weak transcranial direct current stimulation. J Physiol (Lond) 2000;527:633–9.
Nitsche MA, Schauenburg A, Lang N, Liebetanz D, Exner C, Paulis W, et al. Facilitation of implicit motor learning by weak transcranial direct current stimulation of the primary motor cortex in the human. J Cogn Neurosci 2003a;15:619–26.
Nitsche MA, Liebetanz D, Lang N, Antal A, Tergau F, Paulus W. Safety criteria for transcranial direct current stimulation (tDCS) in humans. Clin Neurophysiol 2003b;114:2220–2.
Nitsche MA, Doemkes S, Karakose T, Antal A, Liebetanz D, Lang N, et al. Shaping the effects of transcranial direct current stimulation of the human motor cortex. J Neurophysiol 2007;97:3109–17.
Okamoto M, Matsunami M, Dan H, Kohata T, Kohyama K, Dan I. Prefrontal activity during taste encoding: an fNIRS study. Neuroimage 2006;31:796–806.
Ogata K, Okamoto T, Yamasaki T, Shigeto H, Tobimatsu S. Pre-movement gating of somatosensory-evoked potentials by self-initiated movements: the effects of aging and its implication. Clin Neurophysiol 2009;120:1143–8.
Pesaran B, Nelson MJ, Andersen RA. Dorsal premotor neurons encode the relative position of the hand, eye, and goal during reach planning. Neuron 2006;51:125–34.
Raux M, Xie H, Similowski T, Koski L. Facilitatory conditioning of the supplementary motor area in humans enhances the corticophrenic responsiveness to transcranial magnetic stimulation. J Appl Physiol 2010;108:39–46.
Rizzo V, Siebner HR, Modugno N, Pesenti A, Münchau A, Gerschlager W. Shaping the excitability of human motor cortex with premotor rTMS. J Physiol (Lond) 2003;554:483–95.
Rizzolatti G, Arbib MA. Language within our grasp. Trends Neurosci 1998;21:188–94.
Roche N, Lackmy A, Bussel B, Katz R. Impact of transcranial direct current stimulation on spinal network excitability in humans. J Physiol 2010;587:5653–64.
Schlaug G, Renga V, Nair D. Transcranial direct current stimulation in stroke recovery. Arch Neurol 2008;65:1571–6.
Schluter ND, Rushworth FS, Passinghaml RE, Mills KR. Temporary interference in human lateral premotor cortex suggests dominance for the selection of movements – a study using transcranial magnetic stimulation. Brain 1998;21:785–99.
Shibusawa M, Takeda T, Nakajima K, Ishigami K, Sakatani K. Functional near-infrared spectroscopy study on primary motor and sensory cortex response to clenching. Neurosci Lett 2009;449:98–102.
Stagg CJ, O'Shea J, Kincses ZT, Woolrich M, Matthews PM, Johansen-Berg H. Modulation of movement-associated cortical activation by transcranial direct current stimulation. Eur J Neurosci 2009:1412–23.
Stepniewska I, Preuss TM, Kaas JH. Ipsilateral cortical connections of dorsal and ventral premotor areas in new world owl monkeys. J Comp Neurol 2006;495:691–708.
Tanaka S, Hanakawa T, Honda M, Watanabe K. Enhancement of pinch force on the lower leg by anodal transcranial direct current stimulation. Exp Brain Res 2009;196:459–65.
Taniwaki T, Okayama A, Yoshiura T, Nakamura Y, Goto Y, Kira J, et al. Reappraisal of the motor role of basal ganglia: a functional magnetic resonance image study. J Neurosci 2003;23:3432–8.
Tsuji T, Rothwell JC. Long lasting effects of rTMSand associated peripheral sensory input on MEPs, SEPs and transcortical reflex excitability in humans. J Physiol (Lond) 2002;540:367–76.
Todd G, Butlerb JE, Gandevia SC, Taylor JL. Decreased input to the motor cortex increases motor cortical excitability. Clin Neurophysiol 2006;117:2496–503.
Wolters A, Schmidt A, Schramm A, Zeller D, Naumann M, Kunesch E, et al. Timing-dependent plasticity in human primary somatosensory cortex. J Physiol 2005;565:1039–52.
Zaghi S, Acar M, Hultgren B, Boggio PS, Fregni F. Noninvasive brain stimulation with low-intensity electric currents: putative mechanisms of action for direct and alternating current stimulation. Neuroscientisit 2010;16:285–307.

Clinical Neurophysiology 122 (2011) 708–718

Contents lists available at ScienceDirect

Clinical Neurophysiology

journal homepage: www.elsevier.com/locate/clinph

# Neural responses in the occipital cortex to unrecognizable faces

Takako Mitsudo [a,*], Yoko Kamio [b], Yoshinobu Goto [a,c], Taisuke Nakashima [a], Shozo Tobimatsu [a]

[a] Department of Clinical Neurophysiology, Neurological Institute, Faculty of Medicine, Graduate School of Medical Sciences, Kyushu University, Fukuoka, Japan
[b] Department of Child and Adolescent Mental Health, National Institute of Mental Health, National Center of Neurology and Psychiatry, Kodaira, Japan
[c] Department of Occupational Therapy, Faculty of Rehabilitation, International University of Health and Welfare, Okawa, Fukuoka, Japan

ARTICLE INFO

*Article history:*
Accepted 8 October 2010
Available online 10 November 2010

*Keywords:*
Masked face presentation
ERP
Face inversion effect
Early face sensitivity
P1
N1

HIGHLIGHTS

- The fast face-sensitive process exists prior to the advanced face-specific processing.
- P1 and N1 components at Oz were sensitive to unrecognizable faces.
- P1 grabs rapid holistic detection of the face while N1 detects facial features.

ABSTRACT

*Objective:* Event-related potentials (ERPs) were recorded to examine neural responses to face stimuli in a masking paradigm.
*Methods:* Images of faces (neutral or fearful) and objects were presented in subthreshold, threshold, and suprathreshold conditions (exposure durations of approximately 20, 30 and 300 ms, respectively), followed by a 1000-ms pattern mask. We recorded ERP responses at Oz, T5, T6, Cz and Pz. The effects of physical stimulus features were examined by inverted stimuli.
*Results:* The occipital N1 amplitude (approximately 160 ms) was significantly smaller in response to faces than objects when presented at a subthreshold duration. In contrast, the occipitotemporal N170 amplitude was significantly greater in the threshold and suprathreshold conditions compared with the subthreshold condition for faces, but not for objects. The P1 amplitude (approximately 120 ms) elicited by upright faces in the subthreshold condition was significantly larger than for inverted faces.
*Conclusions:* P1 and N1 components at Oz were sensitive to subthreshold faces, which suggests the presence of fast face-specific process(es) prior to face-encoding. The N170 reflects the robustness of the face selective response in the occipitotemporal area.
*Significance:* Even when presented for a subthreshold duration, faces were processed differently to images of objects at an early stage of visual processing.


## 1. Introduction

Faces are a source of extremely important social signals for humans, and contain complex visual information composed of various low-level visual features. Traditional models of face recognition have generally suggested three primary areas involved in face processing in the human brain (Haxby et al., 2000; Calder and Young, 2005). The fusiform gyrus (fusiform face area; FFA), the lateral occipital cortex (occipital face area; OFA), and the superior temporal sulcus (STS), are all considered to function as face-selective areas in the occipitotemporal cortices. Furthermore, evidence has emerged indicating that these areas exhibit functional specialization; the OFA for facial features, the FFA for identity, and the STS for changeable aspects of faces such as gaze direction (Tsao et al., 2008; Latinus and Taylor, 2006; Pitcher et al., 2007; Rhodes et al., 2009). Several recent event-related potential (ERP) studies examined early face processing using manipulated face images. It was consistently reported that occipital P1/N1 responses occurring between 120 and 180 ms contributed to the detection of facial features, in experimental paradigms using spatially filtered images (Pourtois et al., 2005; Schyns et al., 2007; Nakashima et al., 2008a,b; Obayashi et al., 2009; van Rijsbergen and Schyns, 2009), mosaic faces (Goto et al., 2005), inverted faces (Itier and Taylor, 2002, 2004), and Mooney faces defined by shape-from-shading information (Latinus and Taylor, 2006; George et al., 2005). For

* Corresponding author at: Department of Clinical Neurophysiology, Neurological Institute, Faculty of Medicine, Graduate School of Medical Sciences, Kyushu University, 3-1-1 Maidashi, Higashi-ku, Fukuoka 812-8582, Japan. Tel.: +81 92 642 5543; fax: +81 92 642 5545.
*E-mail addresses:* staka@neurophy.med.kyushu-u.ac.jp, takako.mitsudo.1@ulaval.ca (T. Mitsudo).

1388-2457/$36.00 
doi:10.1016/j.clinph.2010.10.004

faces to be fully recognized, output from several early visual information processing stages must already be integrated (Tarkiainen et al., 2002; Rossion et al., 2003; Latinus and Taylor, 2006). Hence, ERP signatures occurring approximately 100–180 ms after stimulus presentation that are distributed posterior to the N170 are related to 'face categorization' and appear to play a role in mediating holistic and configural face information (Liu et al., 2002; Herrmann et al., 2004).

To explore the early stages of face processing, it is necessary to quantitatively manipulate the level of stimulus recognizability. Various methods have been employed to control subjects' ability to overtly perceive a visual stimulus, including binocular rivalry (Moutoussis and Zeki, 2002), interocular suppression (Jiang and He, 2006; Jiang et al., 2009) and perceptual masking (Bacon-Mace et al., 2005; Martens et al., 2006; Kouider et al., 2008). Perceptual masking has been used to differentiate between automatic and controlled (top-down) processes, and to interrupt higher processing and prevent the overt recognition of stimuli. Recent ERP and functional magnetic resonance imaging (fMRI) studies have reported that viewing masked faces that could not be overtly perceived elicits activity in occipitotemporal areas (Trenner et al., 2004; Martens et al., 2006; Henson et al., 2008; Kouider et al., 2008; Jiang and He, 2006). These studies reported the suppression or enhancement of masked faces was observed in the FFA and OFA, suggesting that neural activity in the occipital cortex does not always correlate with the overt recognition of stimuli as faces.

To address this issue, we examined the role of occipital visual areas in the recognition of briefly presented faces followed by a pattern mask, using different presentation durations to manipulate whether subjects were able to recognize them as faces or not. We systematically presented faces at durations that were under or over the threshold of subjective visibility (determined by adjusting stimulus duration) followed by the presentation of a pattern mask. ERPs from occipital and temporal areas were recorded simultaneously to examine visual activity at early stages of face processing. The study involved two main manipulations: first, to determine the effects of stimulus duration on ERP components, we used subthreshold, threshold, and suprathreshold presentation durations of approximately 20, 30 and 300 ms, respectively. Second, stimulus orientation was inverted to examine whether the physical similarity of the stimuli affected the results.

## 2. Methods

### 2.1. Subjects

Eleven healthy volunteers (five females, aged 20–27 years) participated in two experiments. All subjects were right handed and had normal or corrected-to-normal vision. Written informed consent was obtained from each subject after an explanation of the purpose and procedures to be used in the experiment. The experimental procedures were approved by the Ethics Committee of the Graduate School of Medical Sciences, Kyushu University.

### 2.2. Stimuli and apparatus

Photographs of eight fearful and eight neutral faces from 16 individuals (eight men and eight women) were taken from Matsumoto and Ekman (1988)'s standardized set of Japanese and Caucasian Facial Expressions of Emotion and Neutral Faces (JACFEE and JACNeuF; Fig. 1a). Half of the photographs depicted Asian faces, while the other half were Caucasian faces. All photographs showed a full-frontal view of the face. Eight objects were used as object stimuli (Fig. 1a). We used fearful faces, neutral faces, and non-face objects (as non-target stimuli) with three different stimulus durations in Experiment 1, to study the effect of stimulus duration. In Experiment 2, we used upright and inverted images of fearful faces, neutral faces, and objects presented at a subthreshold duration, to study the effect of inversion. A line drawing of a train was used as a target stimulus (Fig. 1b). All photographs were grayscale, sized 1000 × 660 pixels (visual angle of 17.6° horizontally and 11.7° vertically), and had an average stimulus luminance of 14.8 cd/m$^2$. For a pattern mask, we used a 1024 × 768 pixel noise pattern generated with Adobe Photoshop 7.0. A DELL OptiPlex GX260 computer which mounted VSG2/5 (The Math Works, Cambridge Research Systems Ltd.) controlled stimulus presentation and exposure duration. A 17-inch CRT monitor (SONY Trinitron Multiscan G220) with a refresh rate of 100 Hz was used for stimulus presentation. Electroencephalogram (EEG) and electrooculogram (EOG) data were analyzed using MTS Signal Basic Light 2100 in IBM NetVista A40p (6841-EEJ).

### 2.3. Tasks and procedures

The experiment was conducted in a dimly lit, electrically shielded room. Subjects sat in front of the monitor at a viewing distance of 114 cm. The stimuli were preceded and followed by pattern masks of 1000 ms in duration (Fig. 1b). The target, which appeared in 10% of the trials in each block, was presented for 600 ms to shift subjects' attention away from the non-target stimuli (faces or objects). Subjects were instructed to respond by pressing the button as quickly and accurately as possible when the target stimulus was presented on the screen. Each experimental condition consisted of five blocks of 1000 trials, one block of 200 trials; 60 fearful faces, 60 neutral faces, 60 objects, and 20 targets. The stimuli were presented in a random order.

Experiment 1 was designed to examine whether ERPs elicited by faces that were presented too briefly to be recognizable as faces differed from ERPs elicited by faces presented for a recognizable duration. To this end, we presented images at three different durations: subthreshold (threshold minus 10 ms), threshold (the duration ranged from between 20 to 50 ms between subjects), and suprathreshold (300 ms). In addition, we used fearful faces as well as neutral faces to examine whether emotional content influenced early subthreshold ERP signatures. The order of presentation of the three conditions was fixed for all subjects; subthreshold, threshold and then suprathreshold. This order was used so that the content of the masked stimuli in the subthreshold condition would not have been revealed by allowing participants to experience the suprathreshold condition beforehand.

Experiment 2 was conducted to determine whether ERPs elicited by briefly presented unrecognizable faces resulted from face-specific neural responses rather than from the similarity of the physical features. To this end, we changed the stimulus orientation (upright and inverted) and presented them at the subthreshold duration level. The threshold was determined for each subject using the method of limits with an ascending series (see Table 1). The pattern mask was presented for 1000 ms. Subjects took part in the experiment for 3 days in total; 2 days for Experiment 1 and another 1 day for Experiment 2.

### 2.4. Threshold settings (Table 1)

The threshold setting experiment was conducted to determine the presentation duration at which subjects were able to recognize whether the masked stimuli were faces or objects. In this task, we use an ascending series of trials to prevent subjects from perceiving the content of masked stimuli, because a descending series with a duration exceeding threshold would allow subjects to see that the stimuli contained neutral faces, fearful faces and non-face

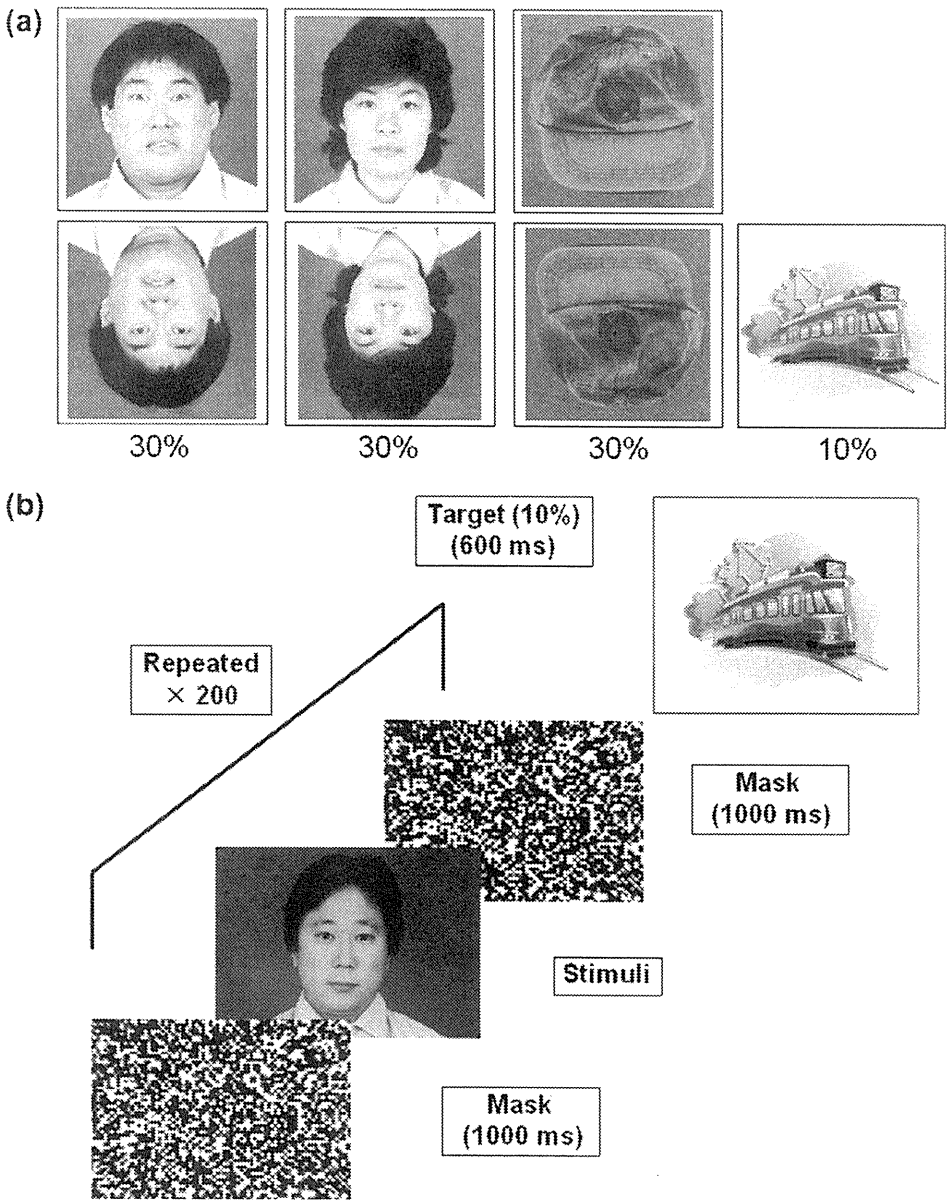


**Fig. 1.** (a) Representative examples of neutral face, fearful face, and object stimuli used in the experiment. (b) Experimental procedures. The faces and objects were followed by a 1000 ms pattern mask without a blank. The target appeared in 10% of the trials in each block, and was presented for 600 ms to draw subjects' attention away from the non-target stimuli.

objects. In each trial, subjects were randomly presented with a neutral face, a fearful face, or an object followed by a pattern mask, and verbally reported which type of stimulus had been presented. The stimulus presentation began with a duration of 10 ms, with duration increased thereafter in 10 ms steps. Stimuli were presented 20–30 times at each stimulus duration. This procedure was followed by Experiments 1 and 2. The threshold-setting stimuli were not used for the ERP experiments. In Table 1, threshold refers to the presentation duration threshold at which subjects first reported that they saw a human-like silhouette (e.g., a silhouette of a human head and shoulders). The total mean and SD represent the average of two measurements.

### 2.5. ERP recordings and data analysis

Because we sought to extract ERP responses from early-stage visual processing areas, we selected five scalp locations (Oz, Cz, Pz, T5 and T6 according to the international 10–20 system) for ERP recording. An electrode on the nose tip was used as a reference. Horizontal and vertical EOG was also recorded, using four electrodes placed over the outer canthi and in the superior and inferior areas of the orbit. Electrode impedance was kept below 5 kΩ throughout recording. ERP and EOG data were filtered with a band-pass filter of 0.05–200 Hz, and sampled at a rate of 1.67 kHz. Averaged waveforms were then low-pass filtered at 30 Hz without phase shifting. For the ERP analysis, stimulus epochs began 60 ms prior to stimulus onset, and continued for 560 ms after. Trials in which eye blinks or other artifacts such α waves (defined as a wave for which voltage exceeded ±50 μV at any electrode) were excluded from the analysis.

We first focused on ERP components measured over occipital areas. At Oz, the first negative peak at about 80 ms after stimulus onset was defined as an 'early negativity' (eN) and the following positive peak at approximately 100 ms after the stimulus onset

**Table 1**
Results of threshold setting in each subject.

| Exp 1 | | Exp 2 | |
|---|---|---|---|
| | Threshold | | Threshold |
| S 1 | 40 | S 1 | 30 |
| S 2 | 30 | S 2 | 40 |
| S 3 | 30 | S 3 | 30 |
| S 4 | 30 | S 4 | 40 |
| S 5 | 40 | S 5 | 30 |
| S 6 | 30 | S 6 | 30 |
| S 7 | 20 | S 7 | 40 |
| S 8 | 30 | S 8 | 30 |
| S 9 | 50 | S 9 | 20 |
| S 10 | 30 | S 10 | 40 |
| S 11 | 40 | S 11 | 20 |
| Mean | 33.6 | Mean | 31.8 |
| SD | 8.1 | SD | 7.5 |
| Total mean | 32.7 | | |
| Total SD | 7.8 | | |

S: subject.

was defined as the occipital P1. The negative peak at approximately 150 ms following the P1 was defined as the occipital N1. We defined the N170 as a negative peak occurring at approximately 170 ms at the occipitotemporal site after stimulus onset. The amplitudes and latencies of the P1 and N1 at Oz and N170 at T5 and T6 were measured using a 60 ms pre-stimulus period as a baseline.

To analyze the latency of electrophysiological responses in Experiment 1, we conducted a three-way repeated measures ANOVA (3 [electrodes: Oz, T5 and T6] × 3 [stimulus types: neutral faces, fearful faces and objects] × 3 [stimulus duration: subthreshold, threshold and suprathreshold]) to ensure that the component recorded at Oz differed from that recorded at T5 and T6. For the amplitude analysis, we conducted a two-way repeated measures ANOVA (3 [stimulus type: neutral faces, fearful faces and objects] × 3 [stimulus duration: subthreshold, threshold and suprathreshold]) for the P1, N1 and the N170, respectively. In Experiment 2, we measured the amplitude and latency of the P1 in each orientation. For the latency and amplitude analyses, we conducted two-way repeated measures ANOVAs for the P1, N1 and N170 (3 [stimulus type: neutral faces, fearful faces and objects] × 2 [stimulus orientation: upright, inverted]). Bonferroni's correction was used for multiple comparisons in a *post hoc* *t*-test.

We further evaluated the time-course of the differences in responses to faces and objects systematically to determine the onset of the face effects. Thus, we analyzed the confidence intervals of ERP differences of faces (neutral/fearful) and objects over time, in accord with the methods of Rousselet et al. (2008). Analyses were performed on the mean amplitudes of responses to faces ((neutral + fearful)/2) and objects of Oz, T5 and T6 in Experiment 1, and the response to upright faces and inverted faces at Oz in Experiment 2. These responses were examined over 51 successive time windows (20 sampling points per 0.6 ms, resulted in 11.4 ms each) across subjects, from the beginning (−60 ms) to the end (560 ms) of each epoch. The differences between the mean response amplitudes for face and object stimuli (or upright and inverted faces in Experiment 2) were calculated across subjects independently for each time-window and condition. The 95% percent confidence interval was then computed (alpha = 0.05). The difference between the two sample means in each time window was considered significant if the 95% confidence interval did not include zero.

In addition, the reproducibility of responses in the subthreshold presentation was examined in five subjects over two recording sessions.

## 3. Results

### 3.1. Subjects' attention

In all experimental conditions, the P300 was exhibited only in response to the target stimulus. This finding confirmed that subjects' attention was not directed to non-target stimuli in either experiment (Fig. 2).

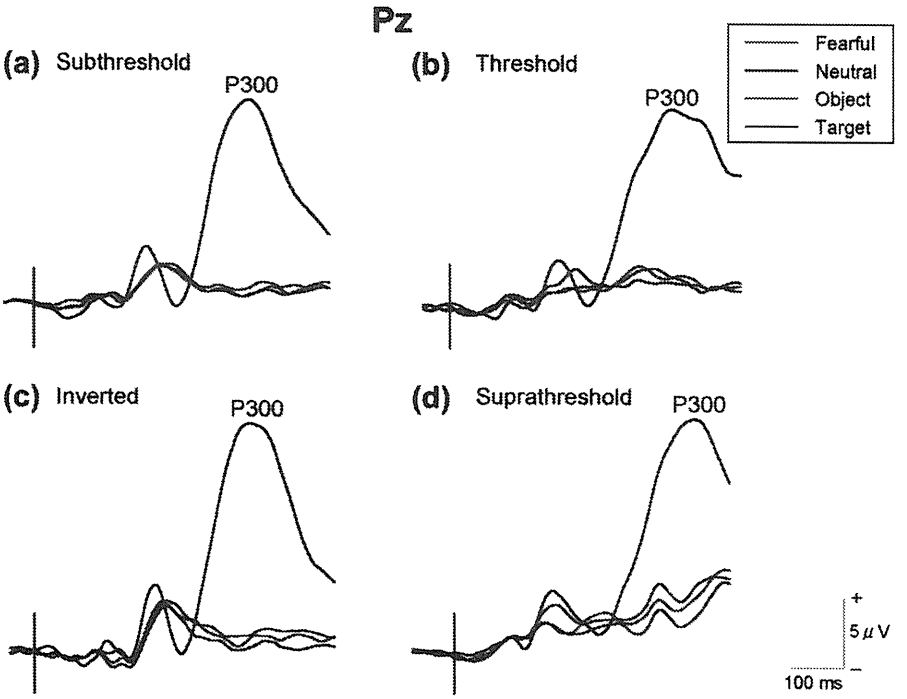


**Fig. 2.** ERP responses to the target stimuli at Pz across the two experimental conditions. The P300 appeared only in response to the target in all stimulus conditions.

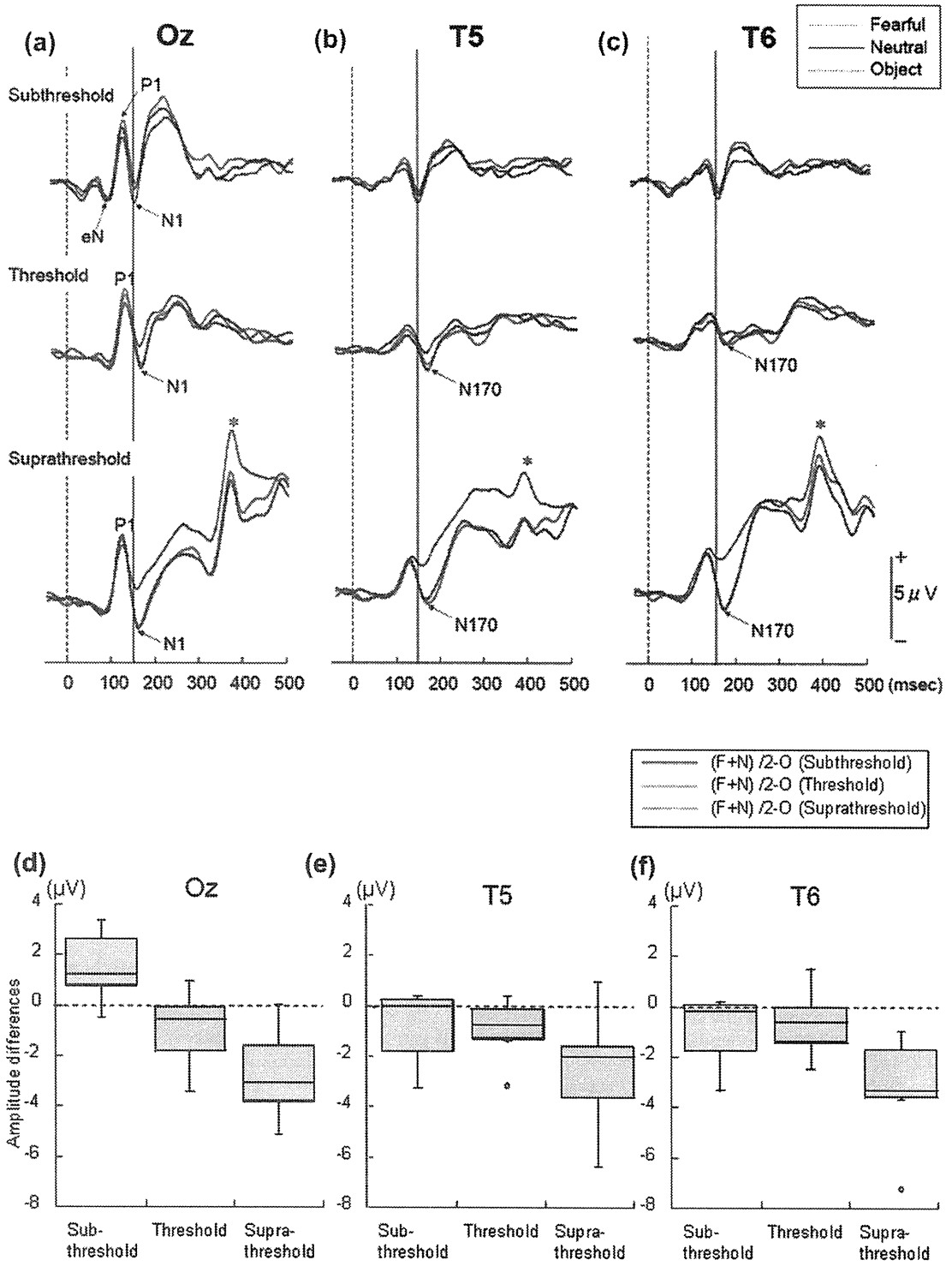


**Fig. 3.** Grand averaged waveforms of the responses at Oz (a), T5 (b) and T6 (c) for neutral faces, fearful faces and objects in the subthreshold, threshold and suprathreshold conditions ($n = 11$). The black line indicates the peak of the occipital N1 response elicited by subthreshold stimuli. The off-response (asterisks) of the visual stimuli was observed at approximately 400 ms (i.e., about 100 ms after the stimulus offset) in the suprathreshold condition. Boxplots of ERP amplitude differences between faces (i.e., (fearful + neutral)/2) and objects in the occipital N1 at Oz (d) and in the temporal N170 at T5 (e) and T6 (f) ($n = 11$). The horizontal line indicates the median values. The boxes extend from the upper to the lower quartile values. The whiskers show the most extreme points within 1.5 times the inter-quartile range. Blue circles indicate outliers. The black dotted lines indicate the point where no amplitude differences between faces and objects were present. The 'faces-objects' difference in the N1 amplitude in the subthreshold condition only appeared at Oz (d). In contrast, 'faces-objects' difference for the N170 amplitude was only evident in the suprathreshold condition. Abbreviations: (F + N)/2-O = (fearful + neutral)/2-object. (For interpretation of the references to colour in this figure legend, the reader is referred to the web version of this article.)

### 3.2. Durations of the subthreshold and threshold levels

Subjects' thresholds differed from 20 to 50 ms. The mean durations were 33.6 ms (SD = 8.1 ms) in Experiment 1 and 31.8 ms (SD = 7.5 ms) in Experiment 2, respectively. The mean subthreshold durations across subjects were 23.6 ms in Experiment 1, and 21.8 ms in Experiment 2 (see Table 1 for details).

### 3.3. Experiment 1

Fig. 3a shows the grand averaged waveforms of the occipital P1 and N1, while Fig. 3b and c represent the grand averaged waveforms of the N170 recorded at T5 and T6. At Oz, the eN, P1 and N1 were examined for the three stimulus durations. The P1 amplitude was not significantly affected by the stimulus type ($F[2, 20] = 3.027$, $p = .096$) or stimulus duration ($F[2, 20] = 2.403$, $p = .134$). Although the interaction did not reach significance ($F[2, 20] = 1.743$, $p = .185$), P1 amplitudes elicited by neutral faces and fearful faces tended to be larger than those elicited by objects in the subthreshold condition (neutral faces vs. objects [$p = .013$], fearful faces vs. objects [$p = .023$]). N1 amplitude differed significantly between faces and objects in the subthreshold condition ($F[2, 20] = 17.275$, $p = .00087$). The N1 amplitude elicited by objects was larger than that for neutral faces and fearful faces in the subthreshold durations (neutral faces vs. objects [$p = .021$], fearful faces vs. objects [$p = .022$]), whereas the N1 for neutral faces and fearful faces was larger than that elicited by objects with presentations at threshold and suprathreshold durations (threshold: neutral faces vs. objects [$p = .031$], fearful faces vs. objects [$p = .034$], suprathreshold: neutral faces vs. objects [$p = .002$], fearful faces vs. objects [$p = .006$], Fig. 3a and Table 2).

For N1 and N170 latencies, the main effect of stimulus duration was significant ($F[2, 20] = 6.107$, $p = .011$). Multiple comparisons revealed that the duration of the N1 in the subthreshold condition was significantly shorter than in the threshold and suprathreshold conditions (subthreshold vs. threshold [$p = .025$], subthreshold vs. suprathreshold [$p = .031$], respectively, See Fig. 3, Tables 2 and 3). Neither the effect of electrode position ($F[2, 20] = 3.224$, $p = .072$) or stimulus type ($F[2, 20] = 1.923$, $p = .177$) were significant. The N170 amplitude did not differ significantly between faces and objects in the subthreshold condition at T5 or T6. However, significant face-object differences appeared when the duration levels increased, shown in the results of the ANOVA given in Tables 2 and 3. Boxplots of the amplitude differences between faces ((fearful + neutral)/2) and objects at Oz, T5 and T6 are shown in Fig. 3d–f. The 'faces-objects' difference for N1 amplitude in the subthreshold condition only appeared at Oz (Fig. 3d). In contrast, the 'faces-objects' difference for the N170 amplitude was only evident in the suprathreshold condition (Fig. 3e and f).

### 3.4. Experiment 2

Grand averaged waveforms of occipital P1 and N1 are shown in Fig 4a. From the waveforms, it can be seen that face-object differences were evident for both the P1 and N1. Interestingly, P1 activity was markedly different to N1 activity, with faces eliciting a larger P1 than object stimuli. ANOVA confirmed the effects on the P1 and N1 of upright stimuli, revealing a significant main effect of orientation on P1 amplitude ($F[2, 20] = 10.293$, $p = .009$, Fig. 4a and b), such that the P1 was significantly larger for the upright condition than for the inverted condition ($p = .009$). In addition, there was a significant interaction of stimulus type × orientation ($F[2, 20] = 7.982$, $p = .014$), such that P1 amplitudes for neutral faces and fearful faces significantly differed between the upright and inverted conditions (neutral faces; $p = .004$, fearful faces; $p = .003$). However, P1 amplitude for the objects was not significantly different between the upright and inverted conditions ($p = .351$). The results revealed no significant main effect of either face orientation or stimulus type on P1 latency.

We found a significant main effect of stimulus orientation on N1 amplitude ($F[1, 10] = 5.433$, $p = .042$, Fig. 4c), such that N1 amplitude was significantly smaller in the upright than the inverted condition ($p = .042$). There was a significant interaction of stimulus type × orientation ($F[2, 20] = 4.874$, $p = .033$). Upright faces and fearful faces elicited smaller amplitudes than inverted faces (neutral faces; $p = .013$, fearful faces; $p = .028$), whereas the N1 amplitude for the objects was not significantly different between upright and inverted conditions ($p = .56$). There was no significant main effect of either image orientation or stimulus type on the latency of responses. In addition, there was no effect of stimulus type or orientation on the N170 amplitude. Finally, there was no significant main effect of electrode on N170 latency. Boxplots of the amplitude differences between faces ((fearful + neutral)/2) and objects of P1 and N1 are shown in Fig. 4b and c. The P1 amplitude difference between faces and objects was only present for the upright stimuli (Fig. 4b). Similarly, the N1 amplitude difference between faces and objects was only present for upright stimuli (Fig. 4c).

### 3.5. Time-course analysis of ERP differences between faces and objects

In Experiment 1, the amplitude of the face-object differences began at 158 ms (time windows of 19) after stimulus onset in the subthreshold and suprathreshold conditions, and 170 ms (time windows of 20) in the threshold condition (Fig. 5). Face-object differences did not appear at any time-windows before N1 or N170

**Table 2**
Mean amplitudes (μV) and latencies (ms) of P1 and N1 for perception of faces (fearful and neutral) and objects.

| Condition | Stimuli | P1 | | N1 | |
|---|---|---|---|---|---|
| | | Amplitude | Latency | Amplitude | Latency |
| Subthreshold | Fearful | 5.4 ± 1.5[a] | 127.2 ± 5.8 | −2.7 ± 1.3[a] | 158.6 ± 7.6 |
| | Neutral | 5.2 ± 1.5[b] | 127.3 ± 6.3 | −2.8 ± 1.4[b] | 156.4 ± 11.4 |
| | Object | 3.7 ± 1.1[a,b] | 125.2 ± 5.9 | −3.6 ± 0.9[a,b] | 163.0 ± 10.1 |
| Threshold | Fearful | 5.1 ± 1.8 | 121.3 ± 8.6 | −1.4 ± 1.3[a] | 169.5 ± 6.4 |
| | Neutral | 4.7 ± 1.5 | 120.9 ± 8.0 | −1.3 ± 0.9[b] | 169.8 ± 6.0 |
| | Object | 5.2 ± 1.9 | 120.6 ± 7.9 | −0.4 ± 1.1[a,b] | 169.0 ± 8.1 |
| Suprathreshold | Fearful | 5 ± 1.7 | 134.1 ± 10.0 | −3.1 ± 2.6[a] | 172.1 ± 7.0 |
| | Neutral | 4.9 ± 1.3 | 124.5 ± 3.3 | −2.6 ± 2.1[b] | 172.7 ± 8.1 |
| | Object | 4.7 ± 0.9 | 126.5 ± 5.4 | 0.3 ± 2.0[a,b] | 173.2 ± 12.1 |

Values are means ± SD. $n = 11$.
[a] Significant effects of multiple comparisons between fearful vs. object ($p < .05$).
[b] Significant effects of multiple comparisons between neutral vs. object ($p < .05$).

**Table 3**
Mean amplitudes (μV) and latencies (ms) of N170 for perception of faces (fearful and neutral) and objects.

| Condition | Stimuli | T5 | | T6 | |
|---|---|---|---|---|---|
| | | Amplitude | Latency | Amplitude | Latency |
| Subthreshold | Fearful | −2.1 ± 0.7 | 159.8 ± 5.8 | −2.3 ± 0.7 | 159.4 ± 5.0 |
| | Neutral | −2.3 ± 0.6 | 157.4 ± 6.1 | −2.4 ± 0.7 | 160.3 ± 7.4 |
| | Object | −2.5 ± 0.8 | 158.4 ± 7.0 | −2.9 ± 0.8 | 159.9 ± 7.4 |
| Threshold | Fearful | −1.8 ± 0.6 | 175.7 ± 6.9 | −2.1 ± 1.6[a] | 176.6 ± 8.7 |
| | Neutral | −1.9 ± 0.4 | 176.7 ± 6.4 | −1.8 ± 1.1[b] | 172.7 ± 8.2 |
| | Object | −1 ± 0.4 | 176.9 ± 9.1 | −0.6 ± 0.8[a,b] | 174.6 ± 9.0 |
| Suprathreshold | Fearful | −2.6 ± 1.9[a] | 174.3 ± 7.5 | −2.5 ± 1.6[a] | 174.1 ± 9.0 |
| | Neutral | −1.7 ± 1.4[b] | 174.3 ± 7.6 | −2.1 ± 1.1[b] | 177.8 ± 7.2 |
| | Object | 0.6 ± 1.4[a,b] | 182.1 ± 9.7 | 0.5 ± 1.1[a,b] | 185.3 ± 10.2 |

Values are means ± SD. $n = 11$.
[a] Significant effects of multiple comparisons between fearful vs. object ($p < .05$).
[b] Significant effects of multiple comparisons between neutral vs. object ($p < .05$).

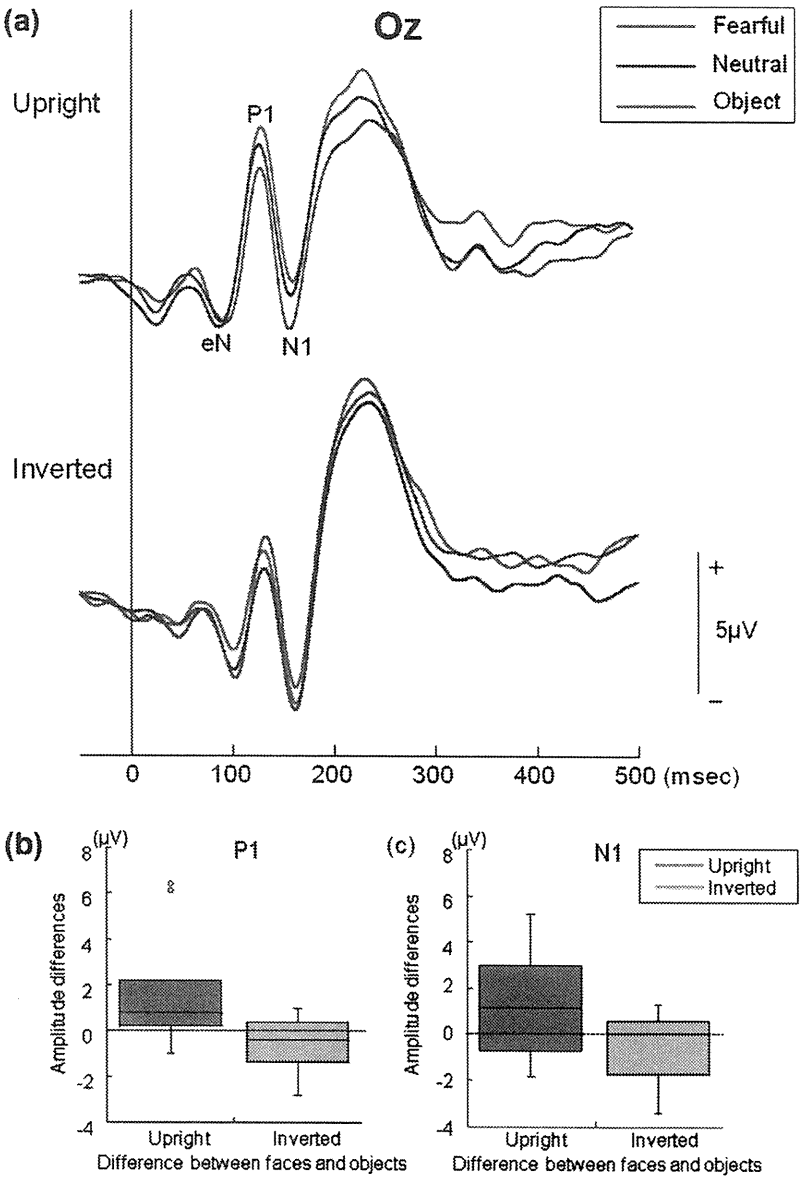


**Fig. 4.** (a) Grand averaged waveforms of the ERP responses for the faces, the fearful faces, and the objects at Oz in the subthreshold upright and inverted conditions in Experiment 2. (b) Boxplots of the ERP amplitude differences between faces (i.e., (fearful + neutral)/2) and objects at occipital P1 ($n = 11$). The P1 amplitude difference between faces and objects was only present for upright stimuli. (c) Boxplots of the ERP amplitude difference between faces (i.e., (fearful + neutral)/2) and objects at occipital N1 ($n = 11$). The N1 amplitude difference between faces and objects was only significant for upright stimuli.

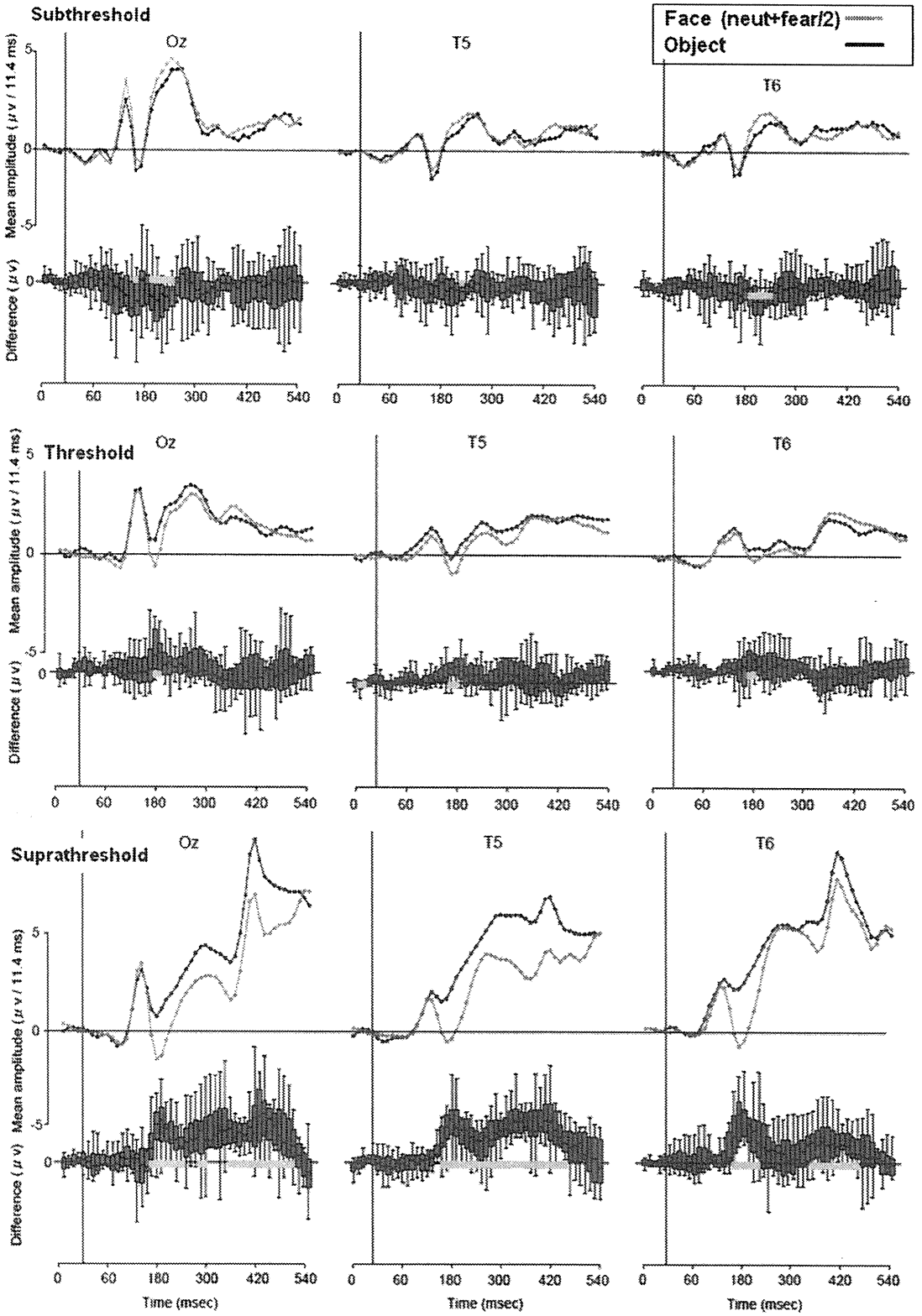


**Fig. 5.** Time-course analysis of the face-object differences among each condition in Experiment 1. For each cell, the red boxplots show the difference between the conditions plotted in red and black circles (each represents the time windows of the mean amplitudes per 20-samplepoints (approximately 11.4 ms) faces and the objects, respectively). The shaded gray area around the red difference boxplots shows the confidence interval of the difference between the two conditions. For each subplot, the horizontal black line indicates the median value. The boxes extend from the upper to the lower quartile values, and each bar represents the minimum and the maximum values. When the confidence interval does not include zero, the difference was significant, as indicated by the thick horizontal bright blue lines. Overall, the time-course analysis indicated significant differences between responses to different image types that started at 158 ms after stimulus onset in the subthreshold and suprathreshold conditions, and at 170 ms in the threshold condition. (For interpretation of the references to colour in this figure legend, the reader is referred to the web version of this article.)